Multi-physics and multi-scale simulations for hydropower and geo-energy

Patrick Zulian, Maria Nestola, Marco Favino, Cyrill von Planta, Rolf Krause
Collaboration with: Jürg Hunziker, Klaus Holliger,
Xiaoqing Chen, Daniel Vogler, Martin Saar

Institute of Computational Science, Università della Svizzera italiana
UNIL - University of Lausanne
ETHZ, GEG

September 13, 2018, Horw, Lucerne

Introduction

Computational energy

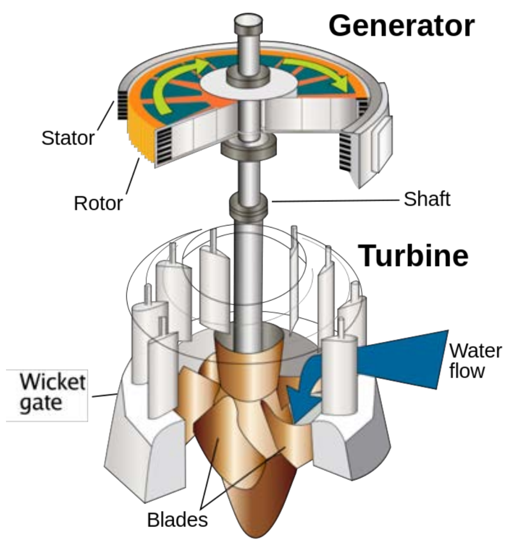

Water turbines

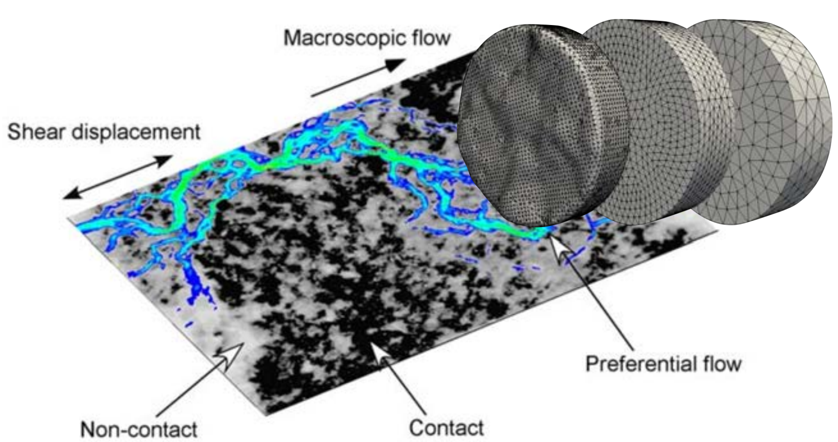

Computational Geophysics

SCCER SoE
SWISS COMPETENCE CENTER for ENERGY RESEARCH
SUPPLY of ELECTRICITY

High-performance computing

Usability

+

Flexibility!

Other applications

Simulation of the heart

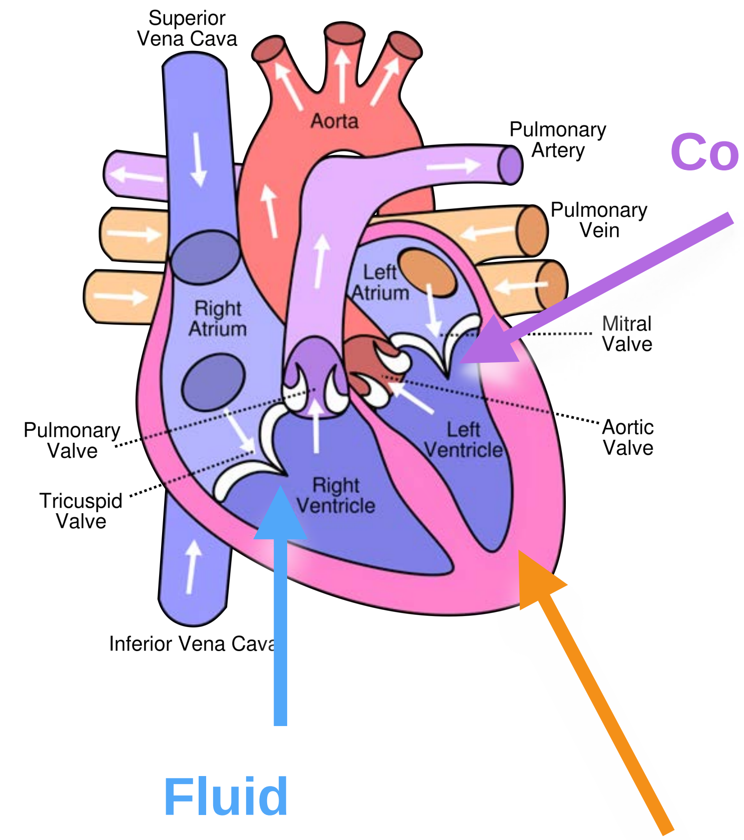

Contact

Fluid

Elasticity/ Electrophysiology

FSI: introduction

Boundary fitted method

- Arbitrary Lagrangian Eulerian (ALE)
- Fluid mesh moves with the solid mesh
- **Accurate** results at FSI interface
- Large displacements → **Distorted fluid grid** → Numerical stability and accuracy
- Meshing, Re-meshing → artificial diffusion

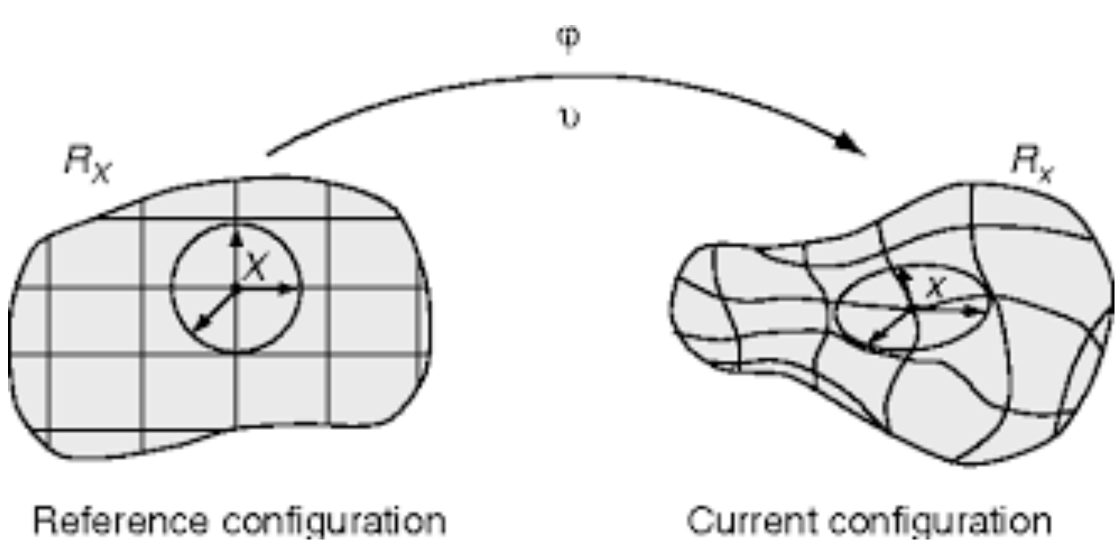

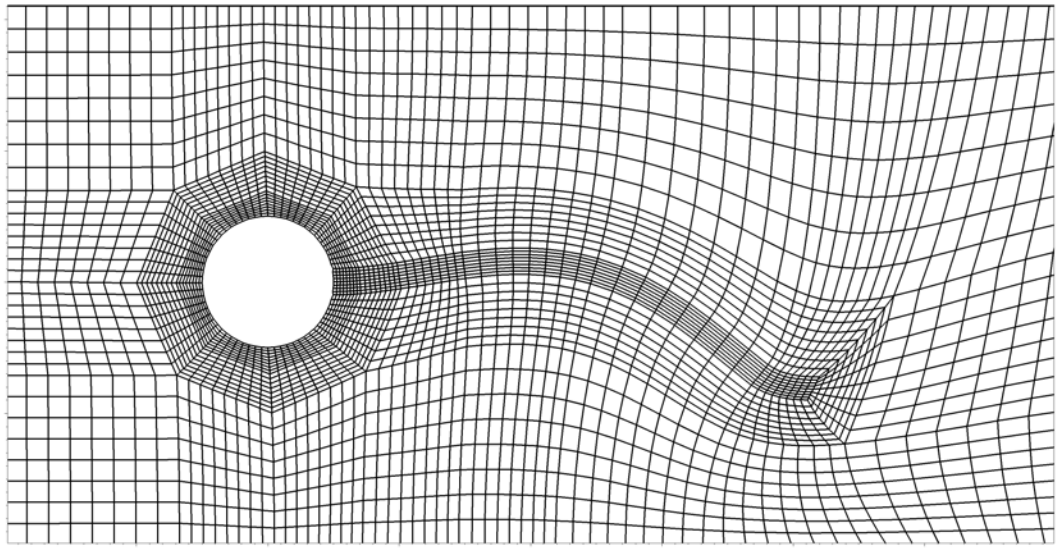

Literature: Jianhai, Dapeng, and Shengquan 1996. Morsi, Yang, Wong, and Das 2007.

FSI: introduction

Fictitious domain method

- Solid phase is embedded in the fluid phase
- **Fixed grid** → Eulerian formulation
- **Greater** grid **resolution** necessary for reproducing similar results
- Different discretizations and software can be easily used together (*e.g.*, Finite Difference and FEM)

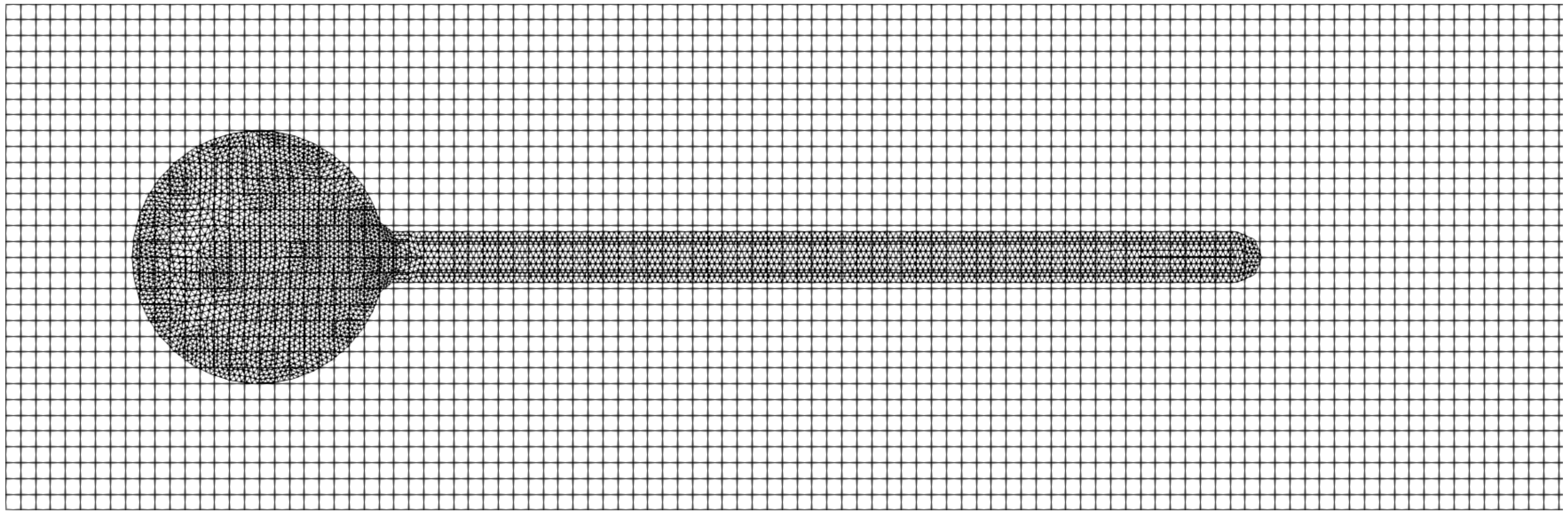

Literature:
1) A fictitious domain/mortar element method for fluid–structure interaction, Baaijens, 2001.
2) A mortar approach for Fluid–Structure interaction problems: Immersed strategies for deformable and rigid bodies, Hesch et al.

FSI: introduction

Find $(\boldsymbol{u}_f, p_f; \boldsymbol{\eta}_s, p_s; \boldsymbol{\lambda}) \subset (\boldsymbol{V}_f \times Q_f \times \boldsymbol{V}_s \times Q_s \times \boldsymbol{L})$ such that

$$\int_{\Omega_f} \rho_f \frac{\partial \boldsymbol{u}_f}{\partial t} \cdot \boldsymbol{v}_f dV + \int_{\Omega_f} \rho_f [(\boldsymbol{u}_f \cdot \nabla)\boldsymbol{u}_f] \cdot \boldsymbol{v}_f dV + \int_{\Omega_f} \boldsymbol{\sigma}_f \cdot \boldsymbol{v}_f dV - \int_{\mathcal{I}} \boldsymbol{\lambda} \cdot \boldsymbol{v}_f dV = 0$$

$$\int_{\Omega_f} q_f \nabla \cdot \boldsymbol{u}_f dV = 0$$

$$\int_{\mathcal{I}} \boldsymbol{\mu} \cdot \Big(\frac{\partial \boldsymbol{\eta}_s}{\partial t} - \boldsymbol{u}_f \Big) dV = 0$$

$$\int_{\widehat{\Omega}_s} \widehat{\rho}_s \frac{\partial^2 \widehat{\boldsymbol{\eta}}_s}{\partial t^2} \cdot \widehat{\boldsymbol{v}}_s + \int_{\widehat{\Omega}_s} \widehat{\boldsymbol{P}}(\widehat{\boldsymbol{F}}) : \nabla \widehat{\boldsymbol{v}}_s dV - \int_{\widehat{\Omega}_s} \widehat{p}_s \widehat{J} \widehat{\boldsymbol{F}}^{-T} : \nabla \widehat{\boldsymbol{v}}_s dV + \int_{\mathcal{I}} \boldsymbol{\lambda} \cdot \widehat{\boldsymbol{v}}_s dV = 0$$

$$\int_{\widehat{\Omega}_s} (\widehat{J} - 1) q_s dV = 0$$

for all $(\boldsymbol{v}_f, q_f; \boldsymbol{v}_s, q_s; \boldsymbol{\mu}) \subset (\boldsymbol{V}_f \times Q_f \times \boldsymbol{V}_s \times Q_s \times \boldsymbol{L})$,where

$$\mathcal{I} = \Omega_s \cap \Omega_f$$

Article: An immersed boundary method based on the variational L² projection approach

M. Nestola, B. Becsek, H. Zolfaghari, P. Zulian, D. Obrist and R. Krause.

Submitted to the proceedings of the 24th International Conference of Domain Decomposition Methods, 2017

FSI: introduction

Find $(\boldsymbol{u}_f, p_f; \boldsymbol{\eta}_s, p_s; \boldsymbol{\lambda}) \subset (\boldsymbol{V}_f \times Q_f \times \boldsymbol{V}_s \times Q_s \times \boldsymbol{L})$ such that

$$\int_{\Omega_f} \rho_f \frac{\partial \boldsymbol{u}_f}{\partial t} \cdot \boldsymbol{v}_f dV + \int_{\Omega_f} \rho_f [(\boldsymbol{u}_f \cdot \nabla)\boldsymbol{u}_f] \cdot \boldsymbol{v}_f dV + \int_{\Omega_f} \boldsymbol{\sigma}_f \cdot \boldsymbol{v}_f dV - \int_{\mathcal{I}} \boldsymbol{\lambda} \cdot \boldsymbol{v}_f dV = 0$$

$$\int_{\Omega_f} q_f \nabla \cdot \boldsymbol{u}_f dV = 0$$

$$\int_{\mathcal{I}} \boldsymbol{\mu} \cdot \left(\frac{\partial \boldsymbol{\eta}_s}{\partial t} - \boldsymbol{u}_f \right) dV = 0$$

$$\int_{\widehat{\Omega}_s} \widehat{\rho}_s \frac{\partial^2 \widehat{\boldsymbol{\eta}}_s}{\partial t^2} \cdot \widehat{\boldsymbol{v}}_s + \int_{\widehat{\Omega}_s} \widehat{\boldsymbol{P}}(\widehat{\boldsymbol{F}}) : \nabla \widehat{\boldsymbol{v}}_s dV - \int_{\widehat{\Omega}_s} \widehat{p}_s \widehat{J} \widehat{\boldsymbol{F}}^{-T} : \nabla \widehat{\boldsymbol{v}}_s dV + \int_{\mathcal{I}} \boldsymbol{\lambda} \cdot \widehat{\boldsymbol{v}}_s dV = 0$$

$$\int_{\widehat{\Omega}_s} (\widehat{J} - 1) q_s dV = 0$$

for all $(\boldsymbol{v}_f, q_f; \boldsymbol{v}_s, q_s; \boldsymbol{\mu}) \subset (\boldsymbol{V}_f \times Q_f \times \boldsymbol{V}_s \times Q_s \times \boldsymbol{L})$,where

$$\mathcal{I} = \Omega_s \cap \Omega_f$$

Article: An immersed boundary method based on the variational L^2 projection approach
M. Nestola, B. Becsek, H. Zolfaghari, P. Zulian, D. Obrist and R. Krause.
Submitted to the proceedings of the 24th International Conference of Domain Decomposition Methods, 2017

FSI: introduction

Find $(\boldsymbol{u}_f, p_f; \boldsymbol{\eta}_s, p_s; \boldsymbol{\lambda}) \subset (\boldsymbol{V}_f \times Q_f \times \boldsymbol{V}_s \times Q_s \times \boldsymbol{L})$ such that

$$\int_{\Omega_f} \rho_f \frac{\partial \boldsymbol{u}_f}{\partial t} \cdot \boldsymbol{v}_f dV + \int_{\Omega_f} \rho_f [(\boldsymbol{u}_f \cdot \nabla)\boldsymbol{u}_f] \cdot \boldsymbol{v}_f dV + \int_{\Omega_f} \boldsymbol{\sigma}_f \cdot \boldsymbol{v}_f dV - \int_{\mathcal{I}} \boldsymbol{\lambda} \cdot \boldsymbol{v}_f dV = 0$$

$$\int_{\Omega_f} q_f \nabla \cdot \boldsymbol{u}_f dV = 0$$

Transfer →

$$\int_{\mathcal{I}} \boldsymbol{\mu} \cdot \Big(\frac{\partial \boldsymbol{\eta}_s}{\partial t} - \boldsymbol{u}_f\Big) dV = 0$$

$$\int_{\widehat{\Omega}_s} \widehat{\rho}_s \frac{\partial^2 \widehat{\boldsymbol{\eta}}_s}{\partial t^2} \cdot \widehat{\boldsymbol{v}}_s + \int_{\widehat{\Omega}_s} \widehat{\boldsymbol{P}}(\widehat{\boldsymbol{F}}) : \nabla \widehat{\boldsymbol{v}}_s dV - \int_{\widehat{\Omega}_s} \widehat{p}_s \widehat{J} \widehat{\boldsymbol{F}}^{-T} : \nabla \widehat{\boldsymbol{v}}_s dV + \int_{\mathcal{I}} \boldsymbol{\lambda} \cdot \widehat{\boldsymbol{v}}_s dV = 0$$

$$\int_{\widehat{\Omega}_s} (\widehat{J} - 1) q_s dV = 0$$

for all $(\boldsymbol{v}_f, q_f; \boldsymbol{v}_s, q_s; \boldsymbol{\mu}) \subset (\boldsymbol{V}_f \times Q_f \times \boldsymbol{V}_s \times Q_s \times \boldsymbol{L})$, where

$$\mathcal{I} = \Omega_s \cap \Omega_f$$

Article: An immersed boundary method based on the variational L^2 projection approach
M. Nestola, B. Becsek, H. Zolfaghari, P. Zulian, D. Obrist and R. Krause.
Submitted to the proceedings of the 24th International Conference of Domain Decomposition Methods, 2017

FSI: introduction

Find $(\boldsymbol{u}_f, p_f; \boldsymbol{\eta}_s, p_s; \boldsymbol{\lambda}) \subset (\boldsymbol{V}_f \times Q_f \times \boldsymbol{V}_s \times Q_s \times \boldsymbol{L})$ such that

$$\int_{\Omega_f} \rho_f \frac{\partial \boldsymbol{u}_f}{\partial t} \cdot \boldsymbol{v}_f dV + \int_{\Omega_f} \rho_f [(\boldsymbol{u}_f \cdot \nabla)\boldsymbol{u}_f] \cdot \boldsymbol{v}_f dV + \int_{\Omega_f} \boldsymbol{\sigma}_f \cdot \boldsymbol{v}_f dV - \int_{\mathcal{I}} \boldsymbol{\lambda} \cdot \boldsymbol{v}_f dV = 0$$

$$\int_{\Omega_f} q_f \nabla \cdot \boldsymbol{u}_f dV = 0$$

Transfer →

$$\int_{\mathcal{I}} \boldsymbol{\mu} \cdot \left(\frac{\partial \boldsymbol{\eta}_s}{\partial t} - \boldsymbol{u}_f \right) dV = 0$$

$$\int_{\widehat{\Omega}_s} \widehat{\rho}_s \frac{\partial^2 \widehat{\boldsymbol{\eta}}_s}{\partial t^2} \cdot \widehat{\boldsymbol{v}}_s + \int_{\widehat{\Omega}_s} \widehat{\boldsymbol{P}}(\widehat{\boldsymbol{F}}) : \nabla \widehat{\boldsymbol{v}}_s dV - \int_{\widehat{\Omega}_s} \widehat{p}_s \widehat{J} \widehat{\boldsymbol{F}}^{-T} : \nabla \widehat{\boldsymbol{v}}_s dV + \int_{\mathcal{I}} \boldsymbol{\lambda} \cdot \widehat{\boldsymbol{v}}_s dV = 0$$

$$\int_{\widehat{\Omega}_s} (\widehat{J} - 1) q_s dV = 0$$

for all $(\boldsymbol{v}_f, q_f; \boldsymbol{v}_s, q_s; \boldsymbol{\mu}) \subset (\boldsymbol{V}_f \times Q_f \times \boldsymbol{V}_s \times Q_s \times \boldsymbol{L})$,where

$$\mathcal{I} = \Omega_s \cap \Omega_f$$

Article: An immersed boundary method based on the variational L[2] projection approach
M. Nestola, B. Becsek, H. Zolfaghari, P. Zulian, D. Obrist and R. Krause.
Submitted to the proceedings of the 24th International Conference of Domain Decomposition Methods, 2017

FSI: staggered approach

Fixed point iteration

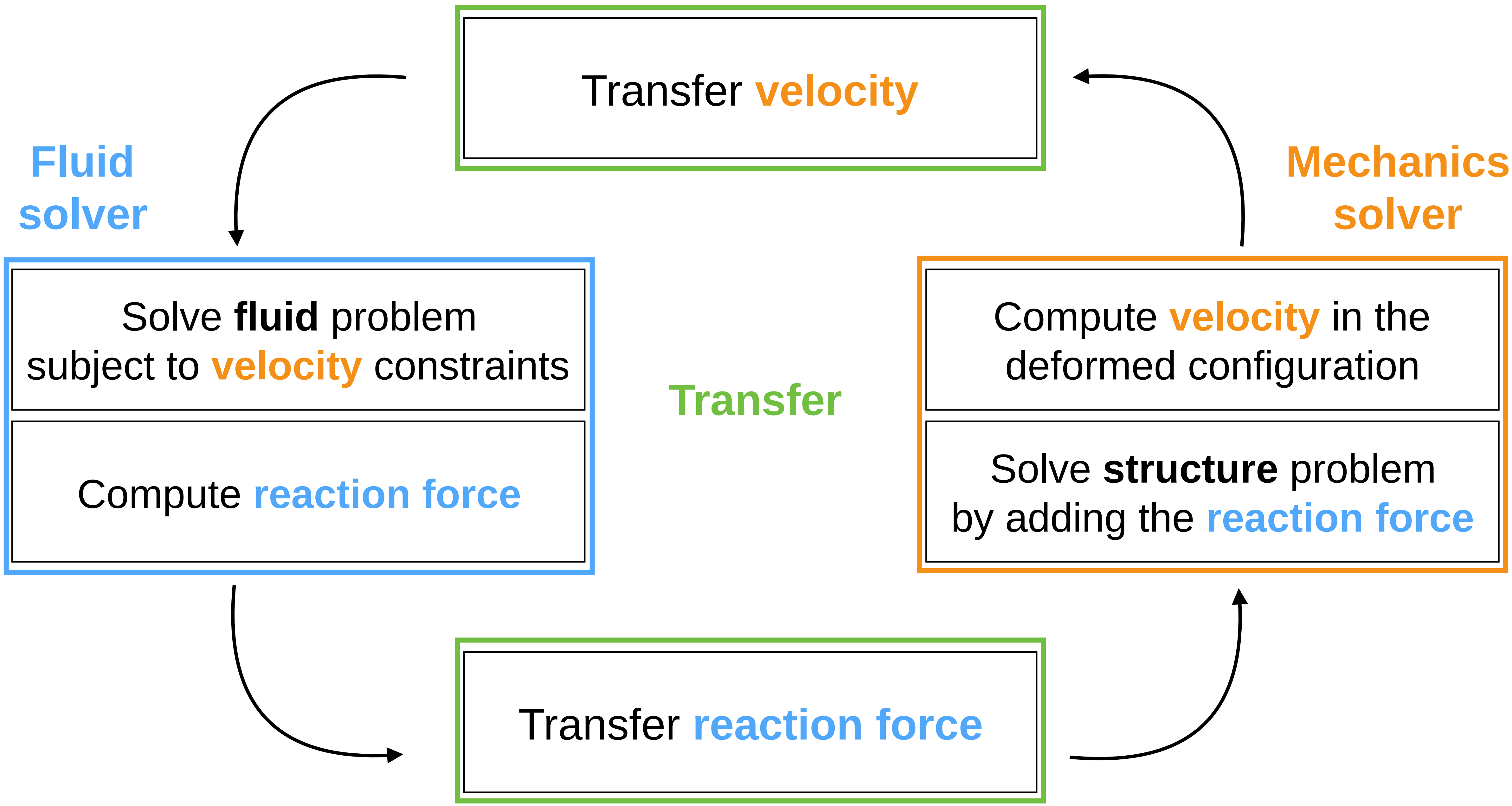

Information transfer

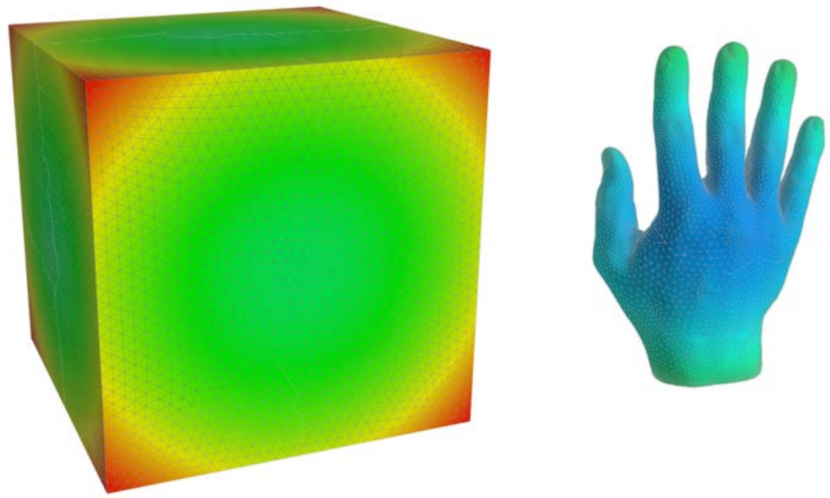

Article: **A parallel approach to the variational transfer of discrete fields between arbitrarily distributed unstructured finite element meshes**, R. Krause and P. Zulian, SIAM Journal of Scientific Computing 2016

Information transfer

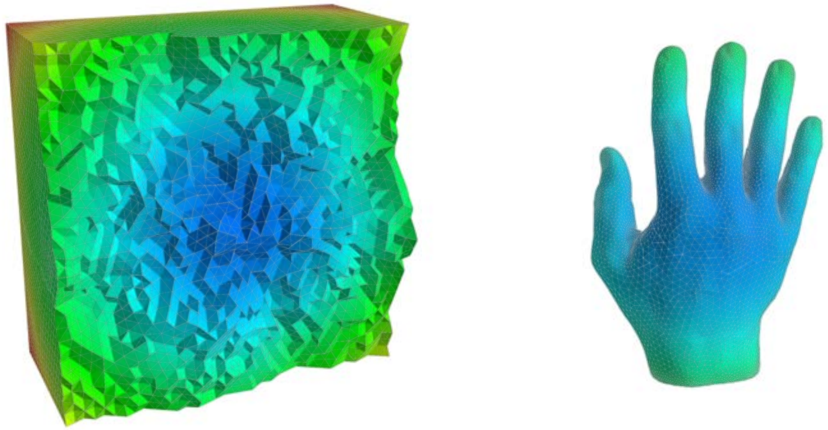

Article: **A parallel approach to the variational transfer of discrete fields between arbitrarily distributed unstructured finite element meshes**, R. Krause and P. Zulian, SIAM Journal of Scientific Computing 2016

Information transfer

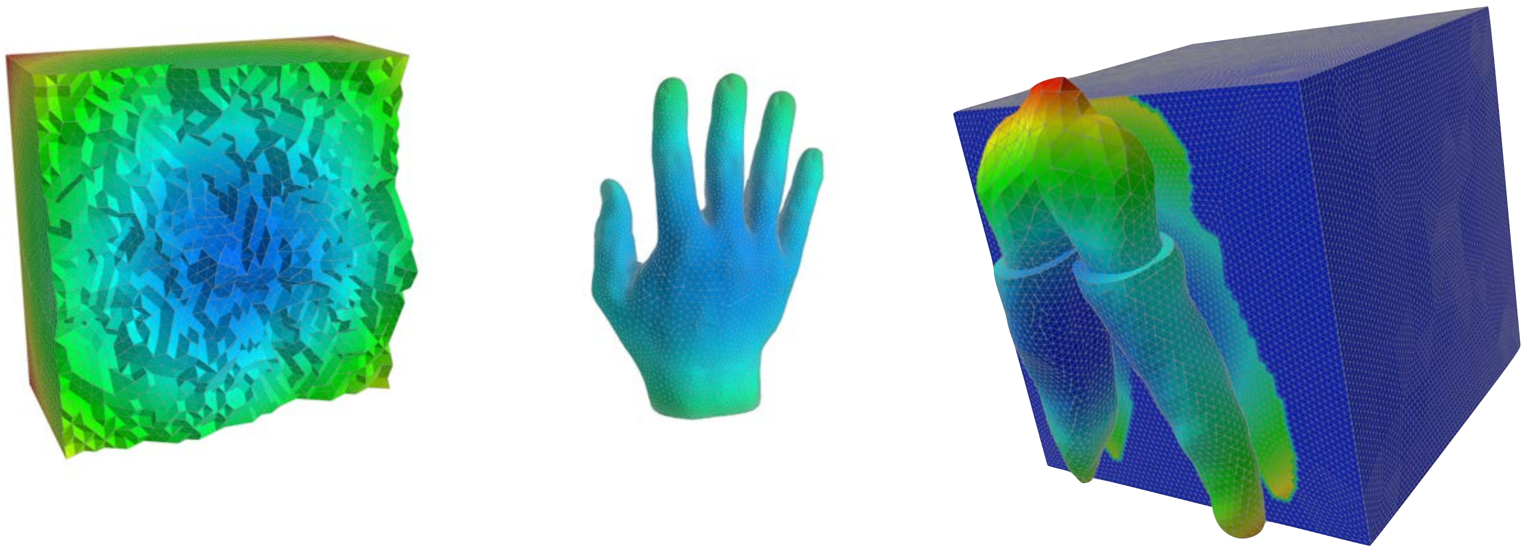

Article: **A parallel approach to the variational transfer of discrete fields between arbitrarily distributed unstructured finite element meshes**, R. Krause and P. Zulian, SIAM Journal of Scientific Computing 2016

Information transfer

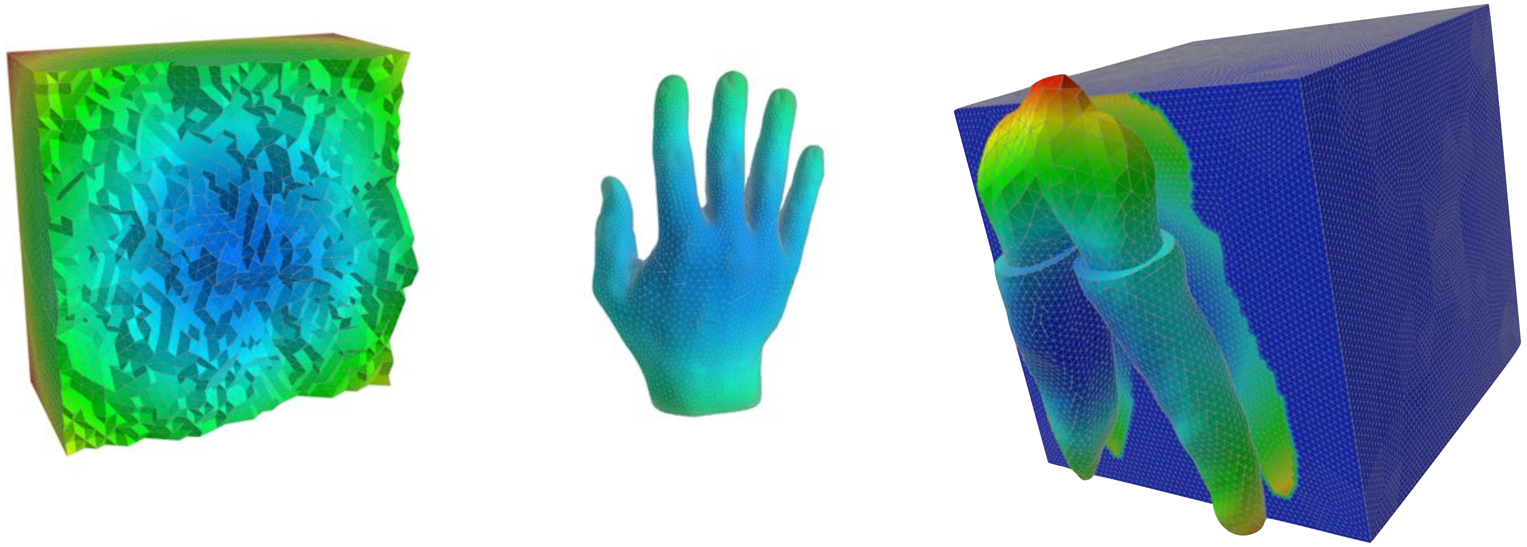

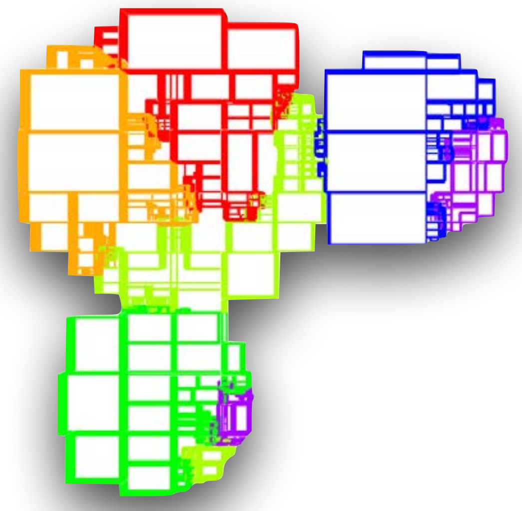

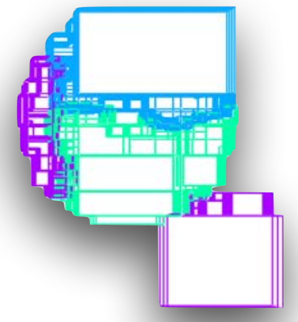

Article: **A parallel approach to the variational transfer of discrete fields between arbitrarily distributed unstructured finite element meshes**, R. Krause and P. Zulian, SIAM Journal of Scientific Computing 2016

Information transfer

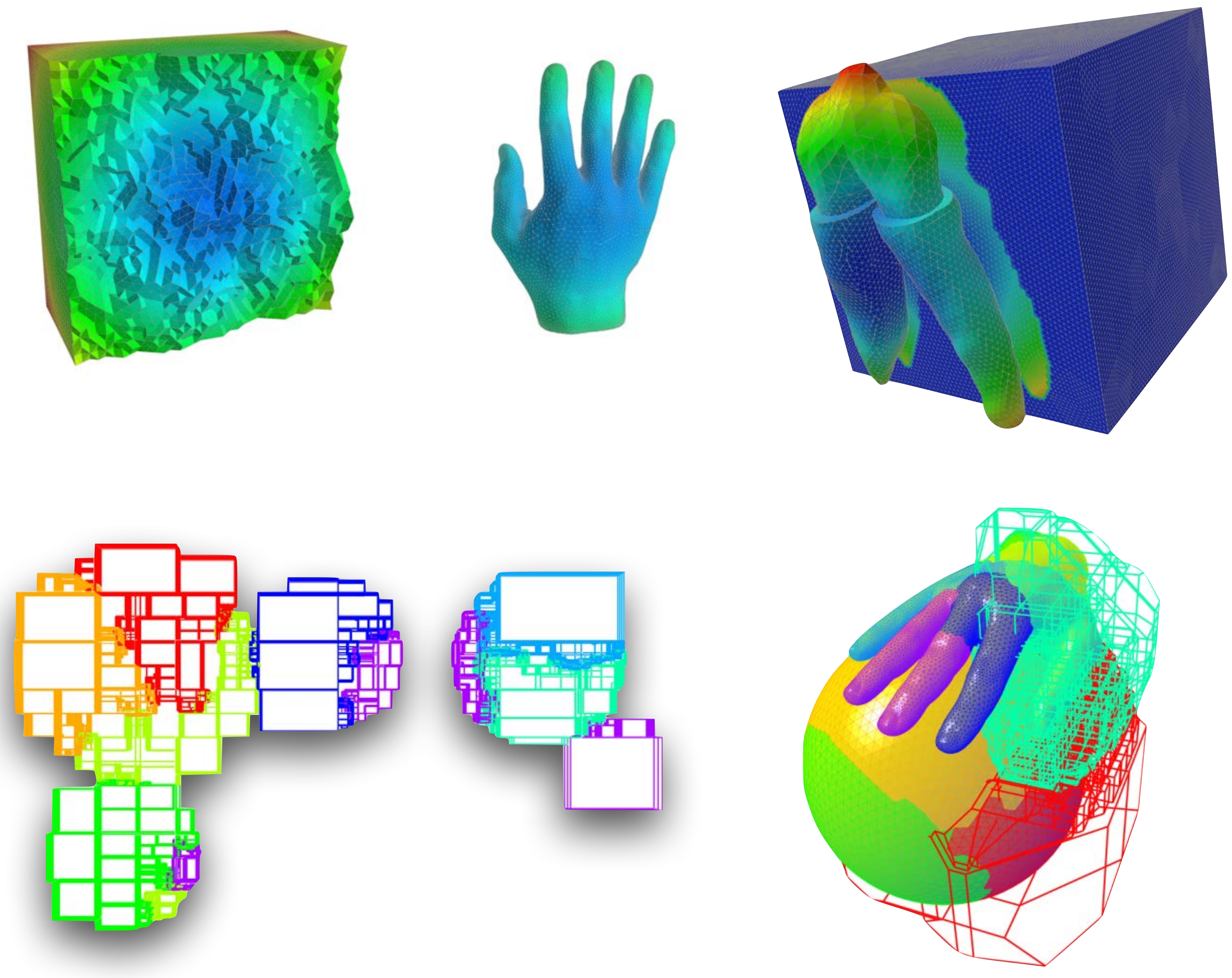

Article: **A parallel approach to the variational transfer of discrete fields between arbitrarily distributed unstructured finite element meshes**, R. Krause and P. Zulian, SIAM Journal of Scientific Computing 2016

Variational transfer

Adjoint

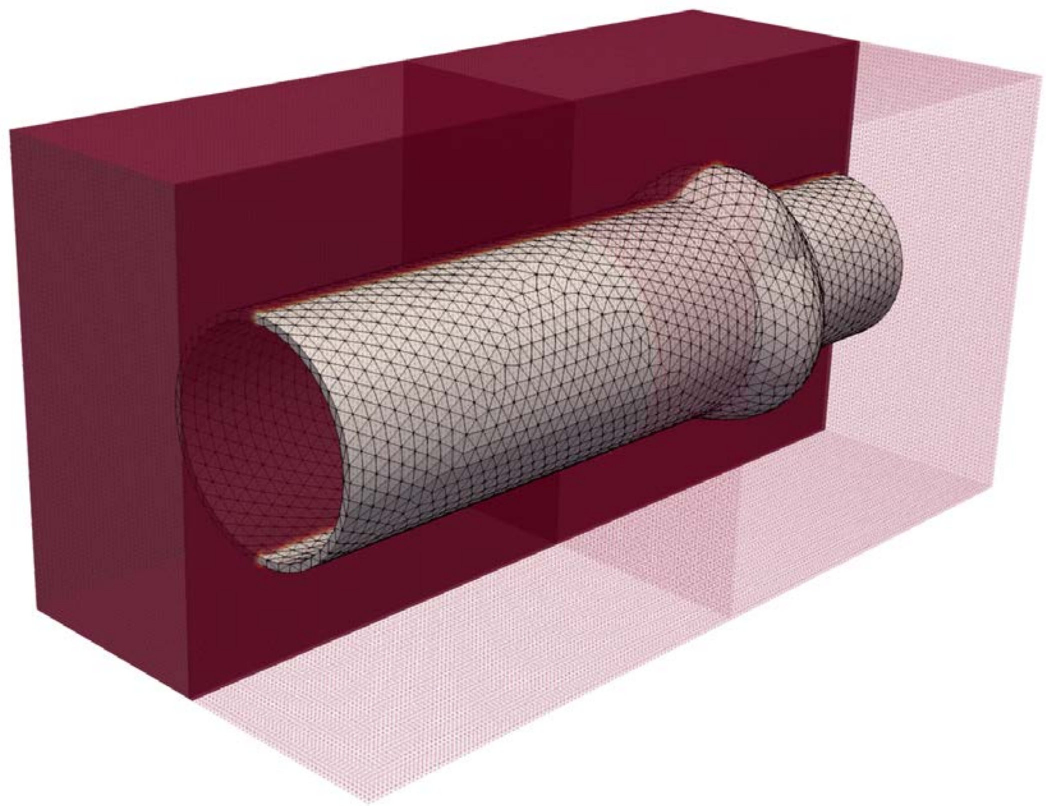

Interpolation

Projection

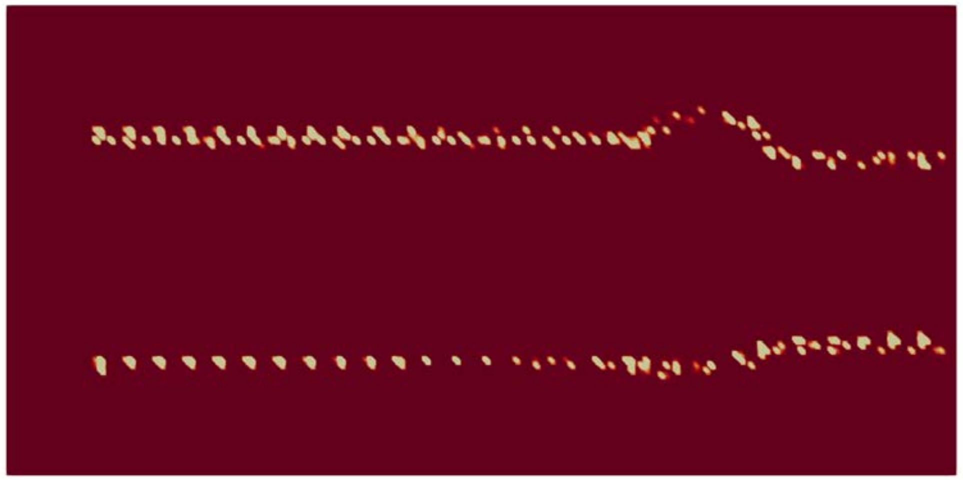

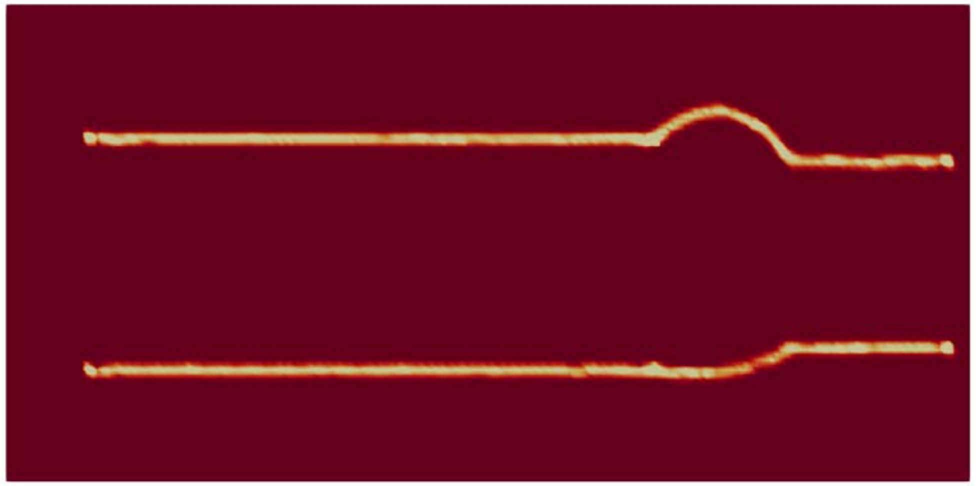

L²-projection

→Optimal, stable, computationally expensive

Interpolation

→Does not pass the patch test, computationally cheaper, simpler for higher-order FE deformations

Variational transfer: mortar projection

- Definition of the L²-projection operator $P: V_h \to W_h$
- For $v_h \in V_h(\mathcal{T}_m)$ find $w_h = P(v_h) \in W_h(T_s)$

$$(P(v_h), \mu_h)_{L^2(I_h)} = (v_h, \mu_h)_{L^2(I_h)} \quad \forall \mu_h \in M_h$$

- Weak-equality condition

$$\int_{I_h} (v_h - P(v_h))\mu_h \, d\boldsymbol{x} = \int_{I_h} (v_h - w_h)\mu_h \, d\boldsymbol{x} = 0 \quad \forall \mu_h \in M_h$$

Literature: Bernardi, Maday and Rapetti 2005.

Variational transfer: mortar projection

Let $\text{span}\{\phi_i\}_{i\in J^V} = V_h$, $\text{span}\{\theta_j\}_{j\in J^W} = W_h$ and $\text{span}\{\psi_k\}_{k\in J^M} = M_h$.

We can now write $v_h = \sum_{i\in J^V} v_i\phi_i$ and $w_h = \sum_{j\in J^W} w_j\theta_j$

Dual Lagrange multipliers (Pseudo-L²-projection)

Literature: Wohlmuth, 1998. Dickopf and Krause 2014.

Variational transfer: mortar projection

Let $\text{span}\{\phi_i\}_{i\in J^V} = V_h$, $\text{span}\{\theta_j\}_{j\in J^W} = W_h$ and $\text{span}\{\psi_k\}_{k\in J^M} = M_h$.

We can now write $v_h = \sum_{i\in J^V} v_i\phi_i$ and $w_h = \sum_{j\in J^W} w_j\theta_j$

and the node-wise contributions

$$\sum_{i\in J^V} v_i \int_{I_h} \phi_i\psi_k \, d\boldsymbol{x} = \sum_{j\in J^W} w_j \int_{I_h} \theta_j\psi_k \, d\boldsymbol{x} \qquad \text{for } k \in J^M$$

$\Longrightarrow \boldsymbol{B}\boldsymbol{v} = \boldsymbol{D}\boldsymbol{w}$ with $b_{ik} = \int_{I_h} \phi_i\psi_k d\boldsymbol{x}$, $d_{jk} = \int_{I_h} \theta_j\psi_k d\boldsymbol{x}$

Dual Lagrange multipliers (Pseudo-L^2-projection)
Literature: Wohlmuth, 1998. Dickopf and Krause 2014.

Variational transfer: mortar projection

Let $\text{span}\{\phi_i\}_{i\in J^V} = V_h$, $\text{span}\{\theta_j\}_{j\in J^W} = W_h$ and $\text{span}\{\psi_k\}_{k\in J^M} = M_h$.

We can now write $v_h = \sum_{i\in J^V} v_i \phi_i$ and $w_h = \sum_{j\in J^W} w_j \theta_j$

and the node-wise contributions

$$\sum_{i\in J^V} v_i \int_{I_h} \phi_i \psi_k \, d\boldsymbol{x} = \sum_{j\in J^W} w_j \int_{I_h} \theta_j \psi_k \, d\boldsymbol{x} \qquad \text{for } k \in J^M$$

$$\implies \boldsymbol{B}\boldsymbol{v} = \boldsymbol{D}\boldsymbol{w} \quad \text{with} \quad \boxed{b_{ik} = \int_{I_h} \phi_i \psi_k d\boldsymbol{x}\,,\; d_{jk} = \int_{I_h} \theta_j \psi_k d\boldsymbol{x}}$$

Dual Lagrange multipliers (Pseudo-L^2-projection)
Literature: Wohlmuth, 1998. Dickopf and Krause 2014.

From intersection to quadrature rule

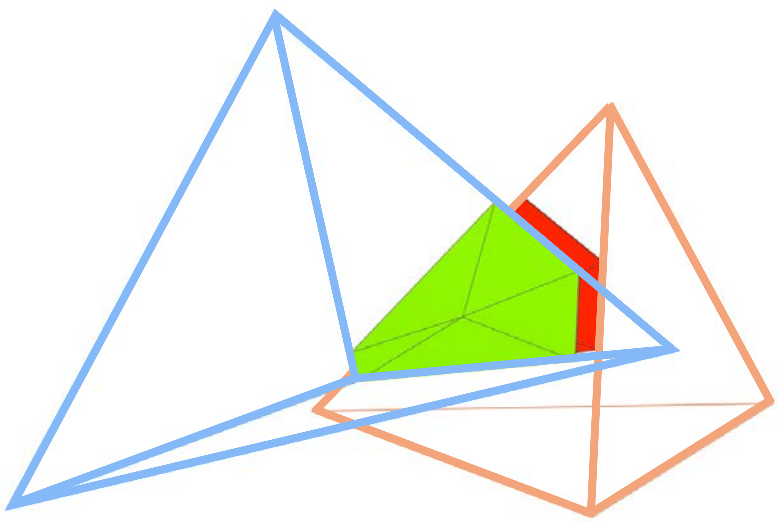

Surface normal projection

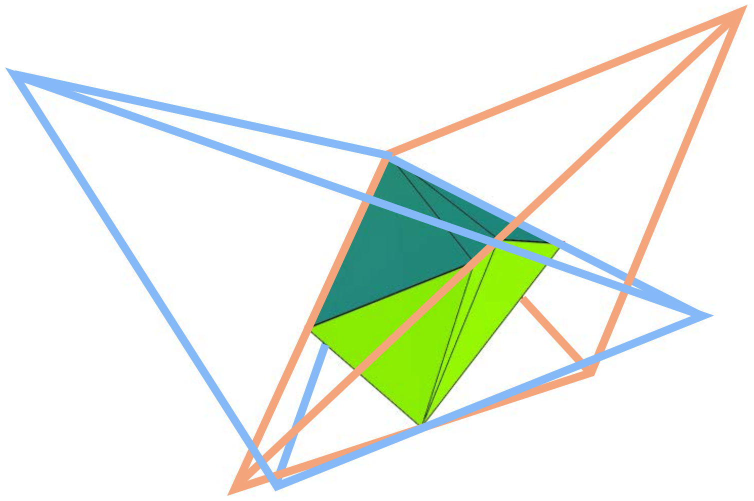

Volume intersection 3D

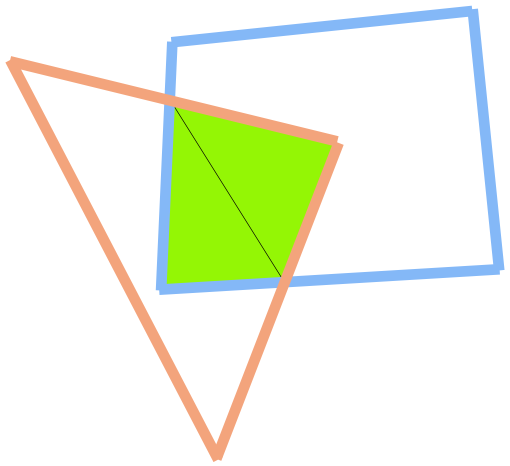

Volume intersection 2D

From intersection to quadrature rule

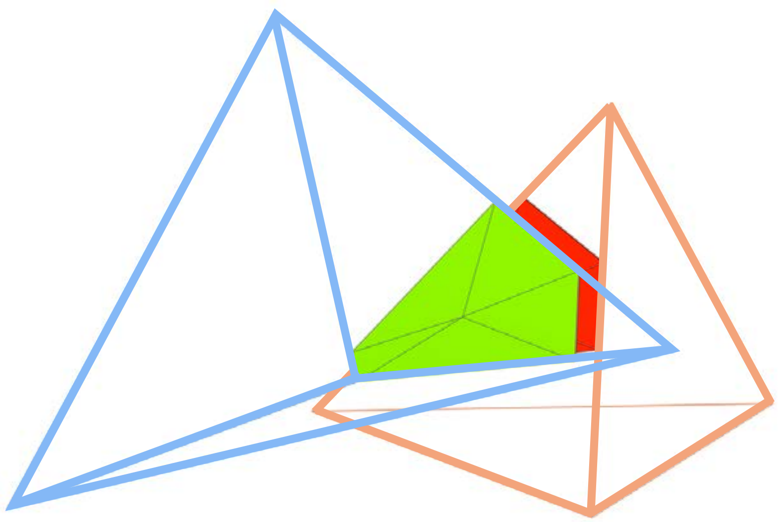

Surface normal projection

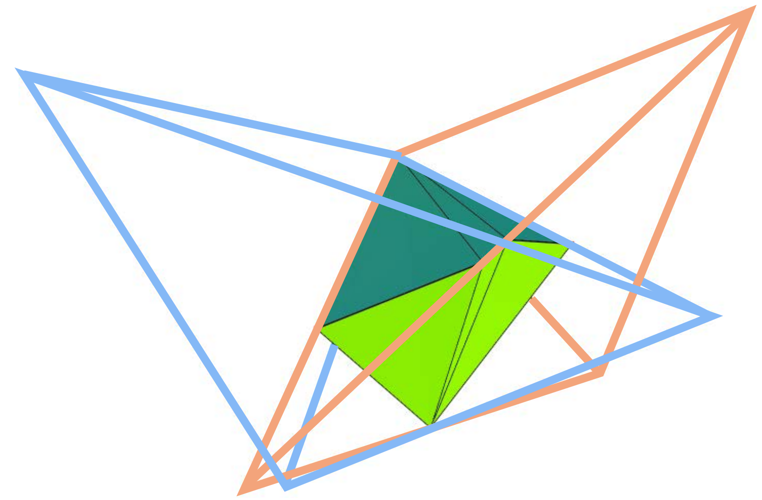

Volume intersection 3D

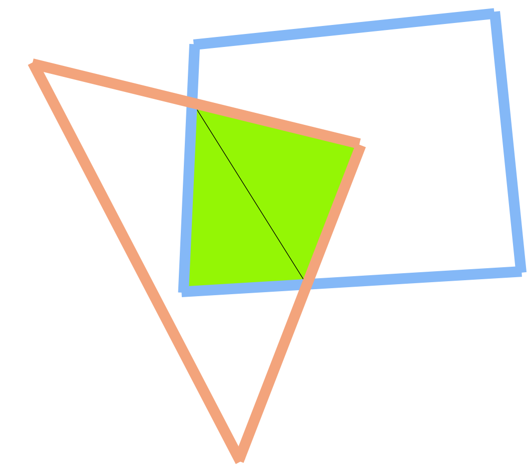

Volume intersection 2D

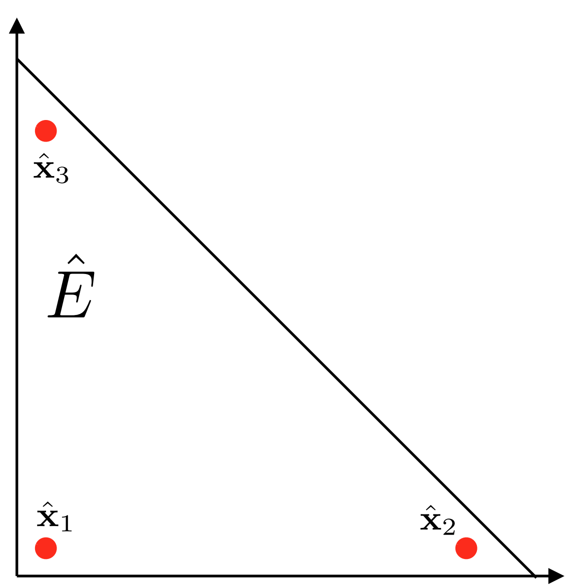

Reference element

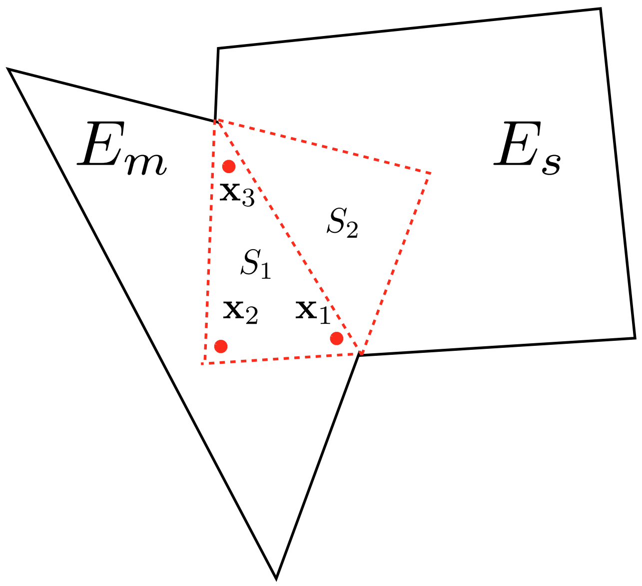

Physical coordinates

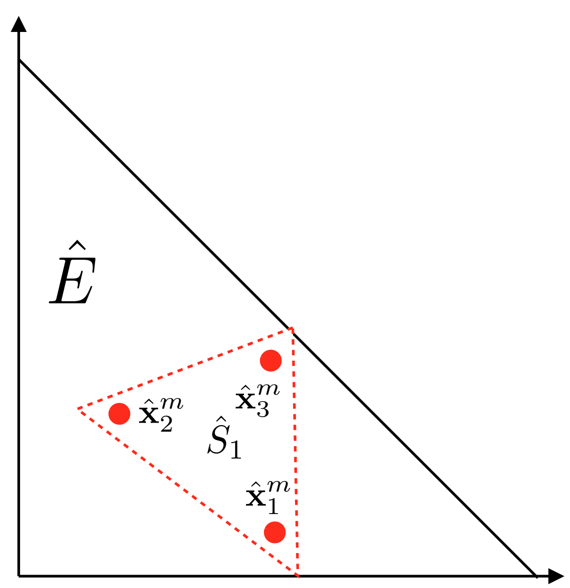

Reference element

Weak scaling (volume projections)

Experiments:

- **Small 10 000** elements per process
- **Large 150 000** elements per process
- Output is **x4**

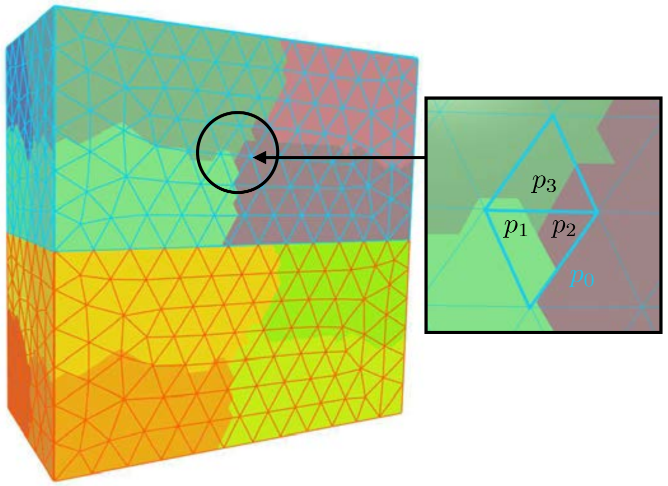

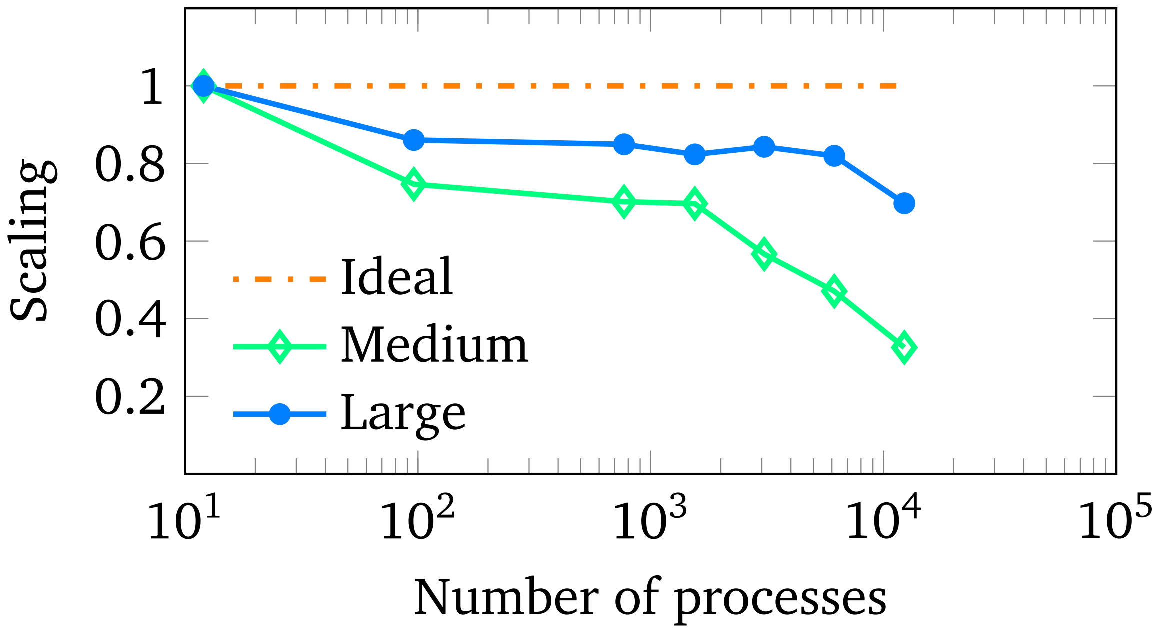

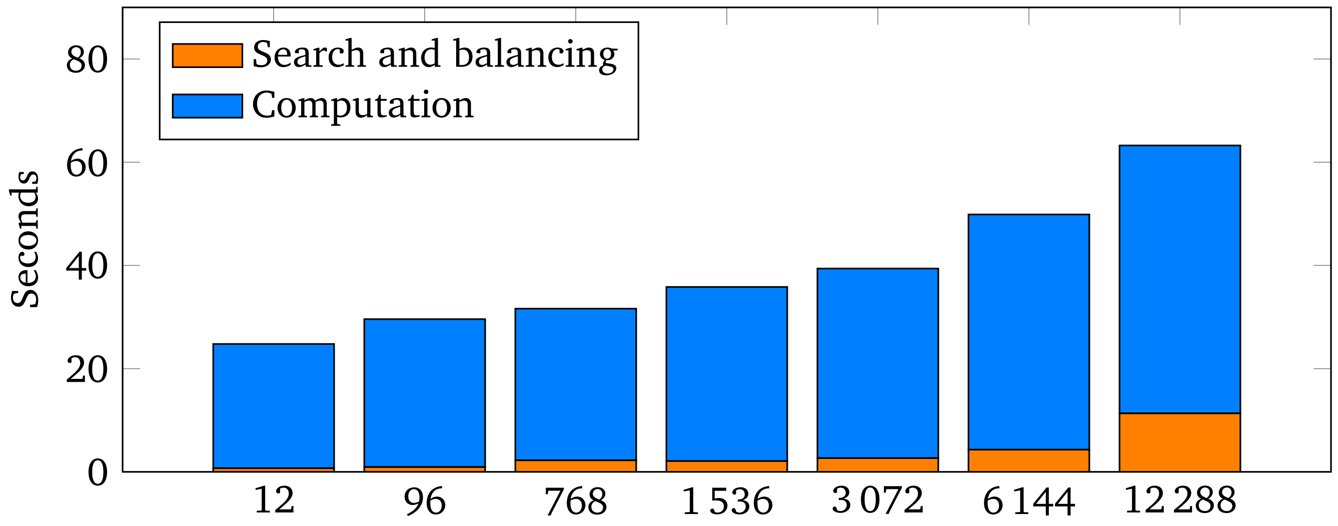

Weak scaling is measured as (time base experiment)/(time experiment)

Validation: FSI

Discretisation error

- L^2-convergence

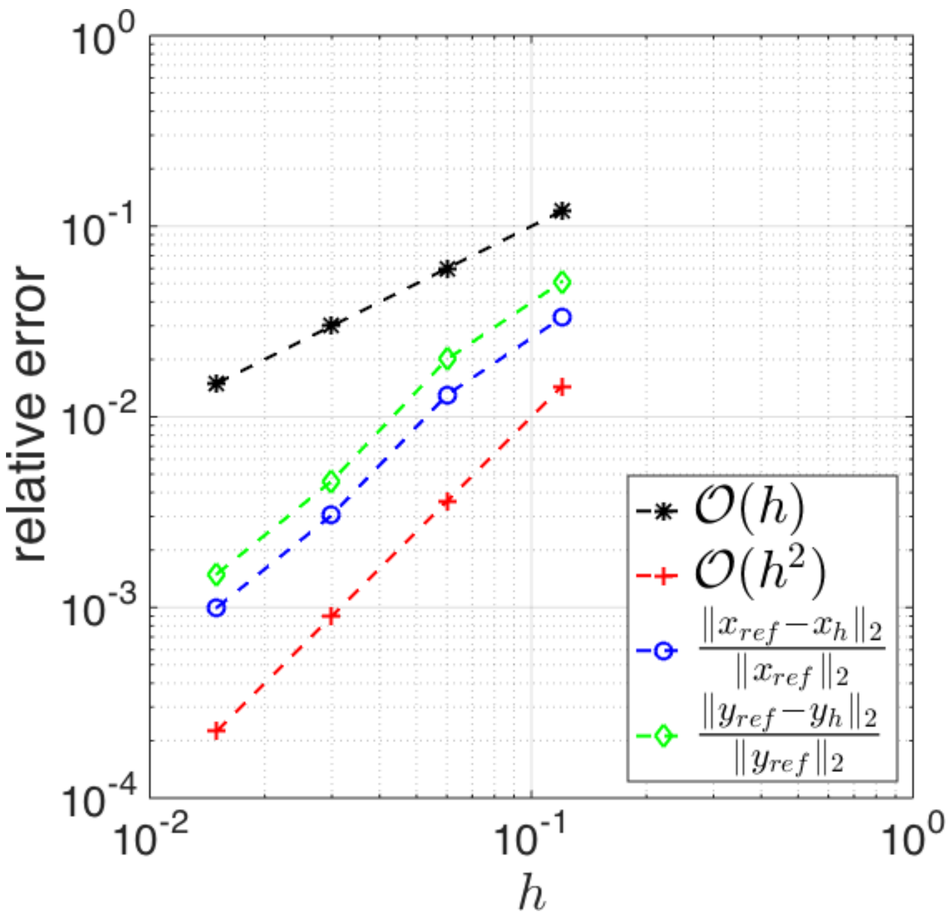

Solid displacement

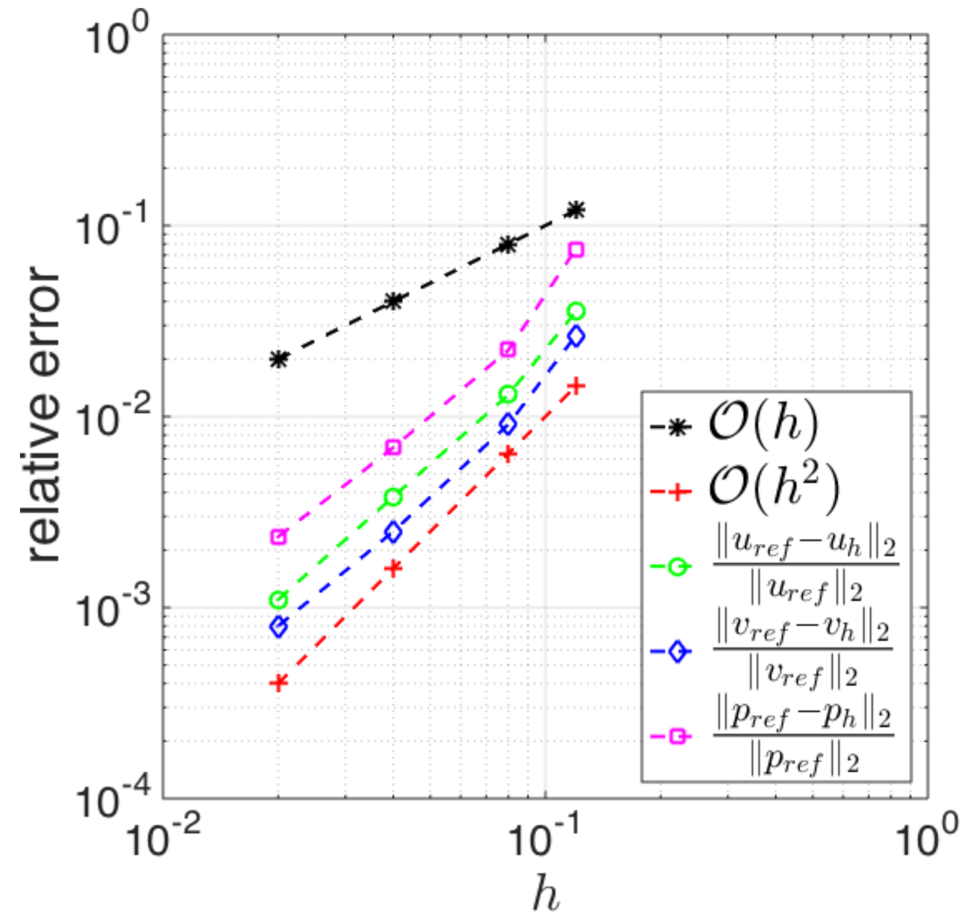

Fluid velocity

Validation: FSI

Free falling rigid cylinder

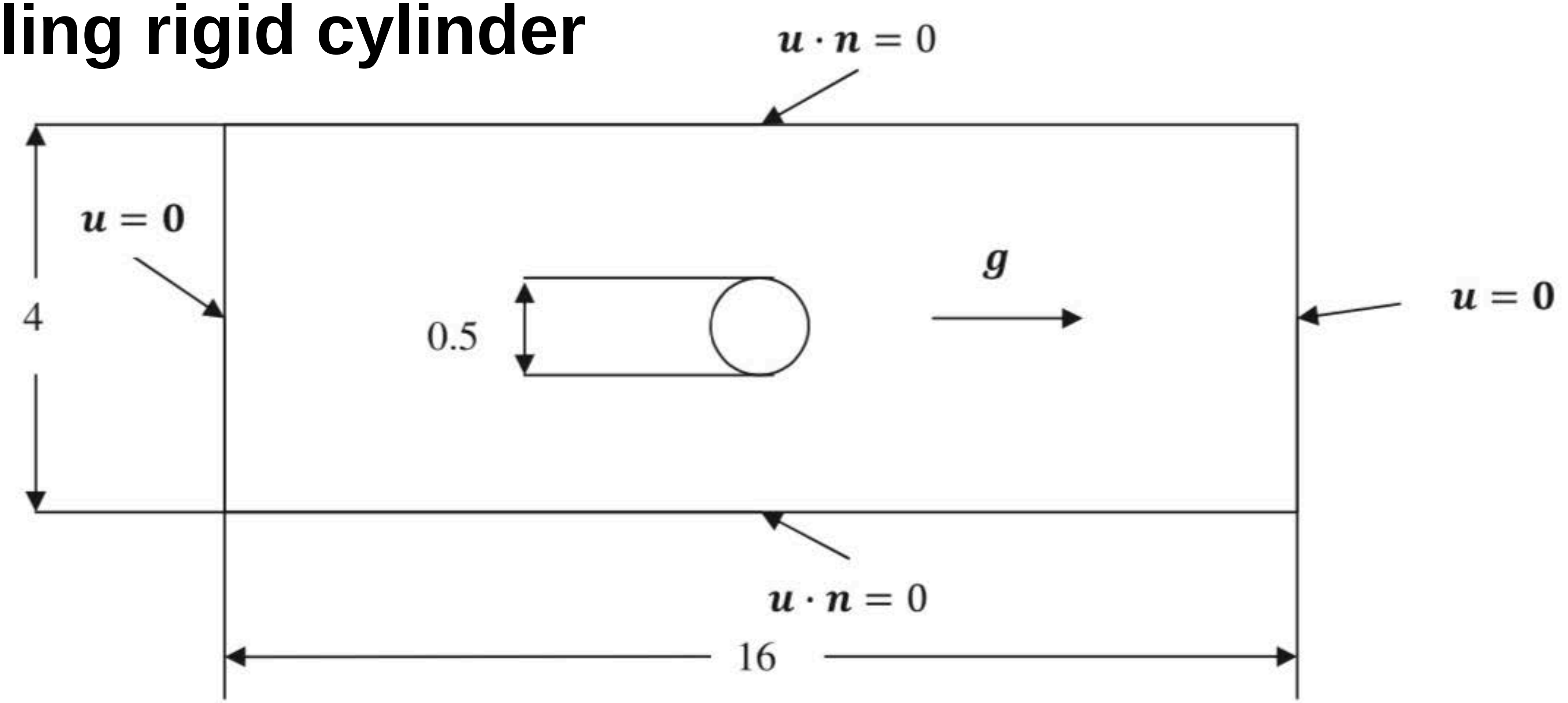

Fluid density

$$\rho_f = 1.0\,[g/cm^3]$$

Newtonian Fluid

$$\sigma_f = -pI + \mu_f \frac{(\nabla^T v_f + \nabla v_f)}{2}$$

$$\mu_f = 1.0\, dyne/cm^2 s$$

Solid density

$$\rho_s = 1.20\,[g/cm^3]$$

Linear Elastic

$$\mu_s = 3846.1538\, dyne/cm^2$$

Literature: Gil, Antonio J., et al. J. Computational Physics 229 (2010): 8613-8641.

Validation: FSI

Free falling rigid cylinder

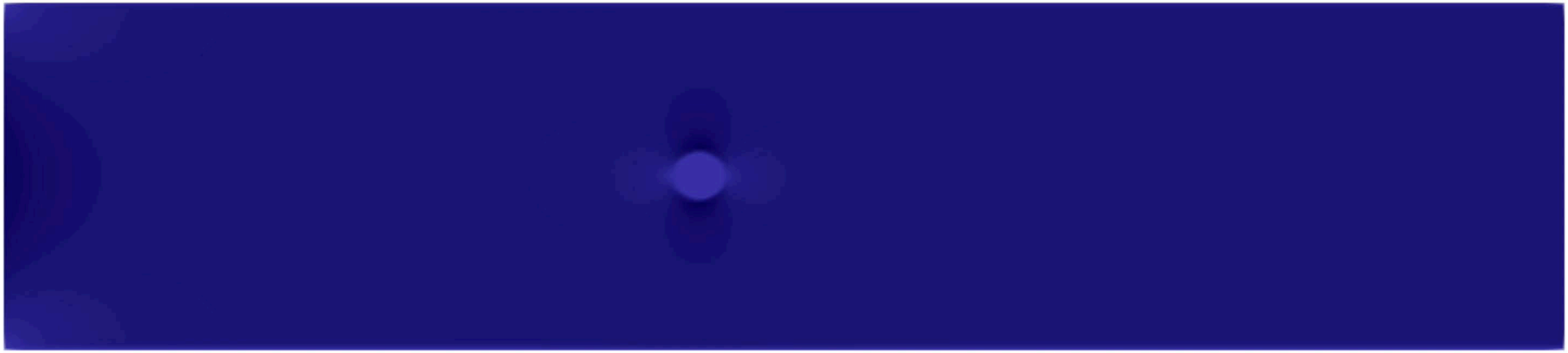

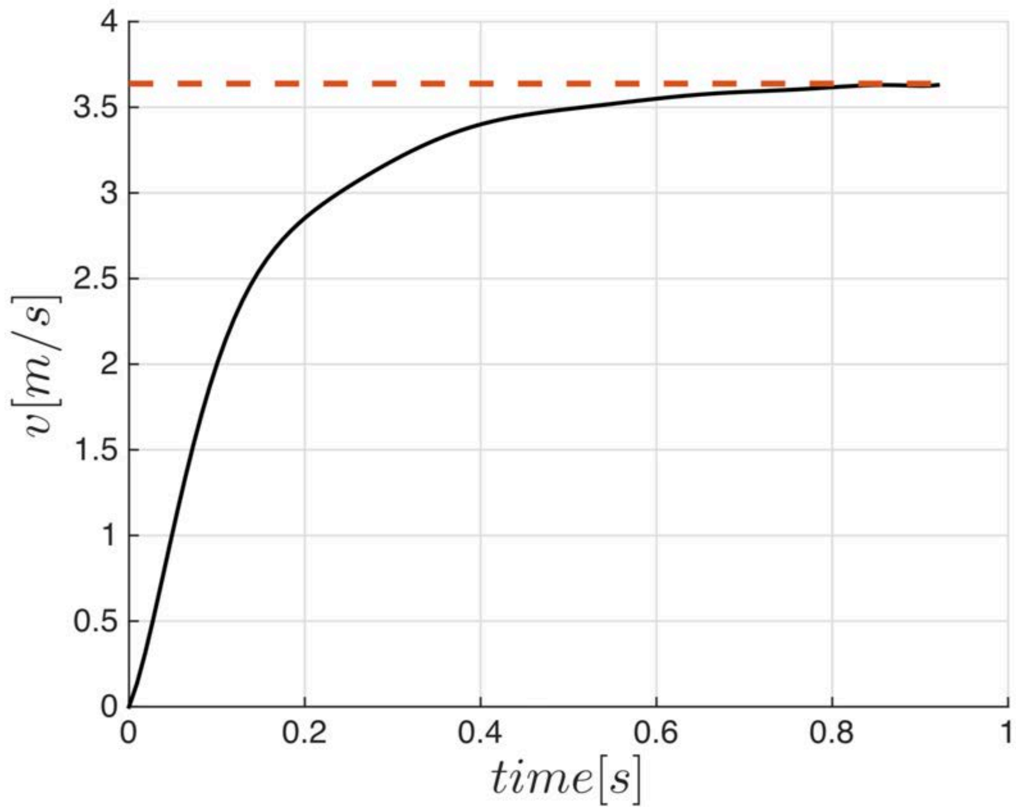

Terminal Velocity

$$\frac{(\rho_s - \rho_f) g a^2}{4\mu}\left[\ln\left(\frac{L}{a}\right) - 0.9157 + 1.7244\left(\frac{a}{L}\right)^2 - 1.7302\left(\frac{a}{L}\right)^4\right]$$

Validation: FSI

Free falling rigid cylinder

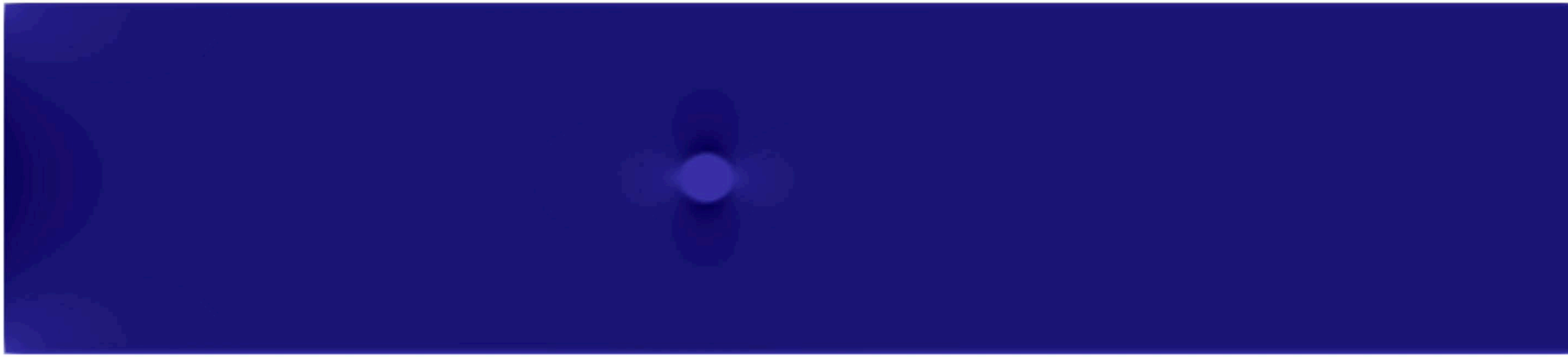

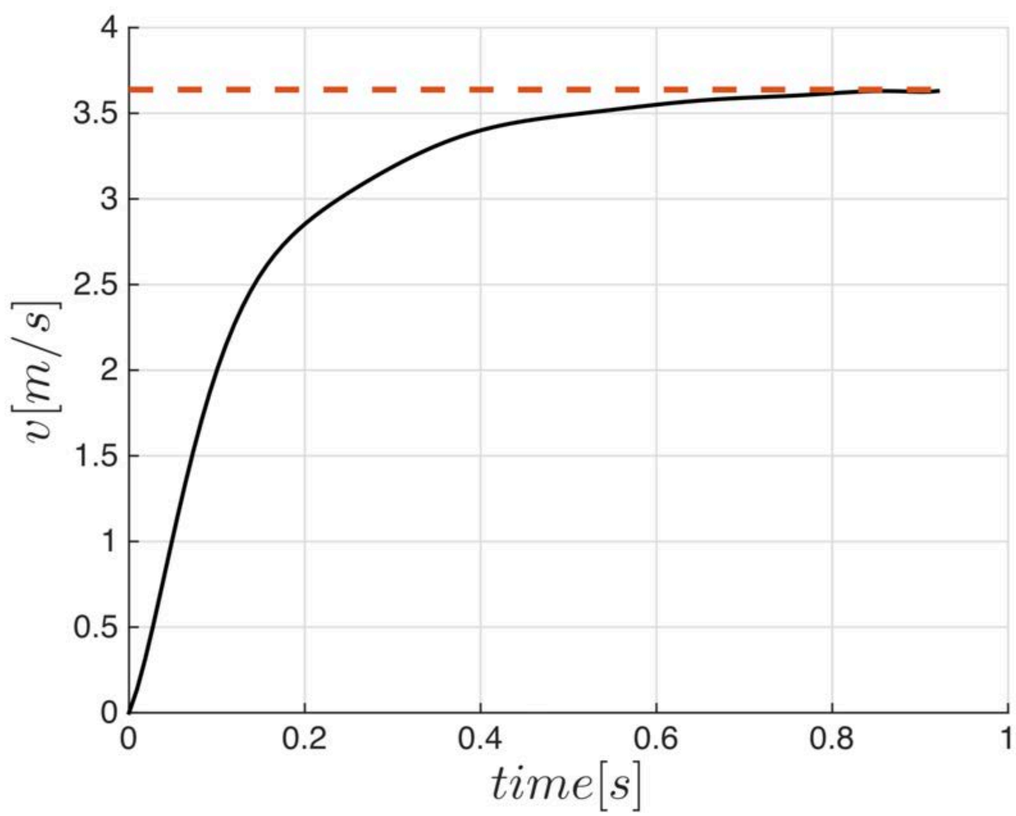

Terminal Velocity

$$\frac{(\rho_s - \rho_f)ga^2}{4\mu}\left[\ln\left(\frac{L}{a}\right) - 0.9157 + 1.7244\left(\frac{a}{L}\right)^2 - 1.7302\left(\frac{a}{L}\right)^4\right]$$

Mesh-tying and FSI on idealised turbines (1)

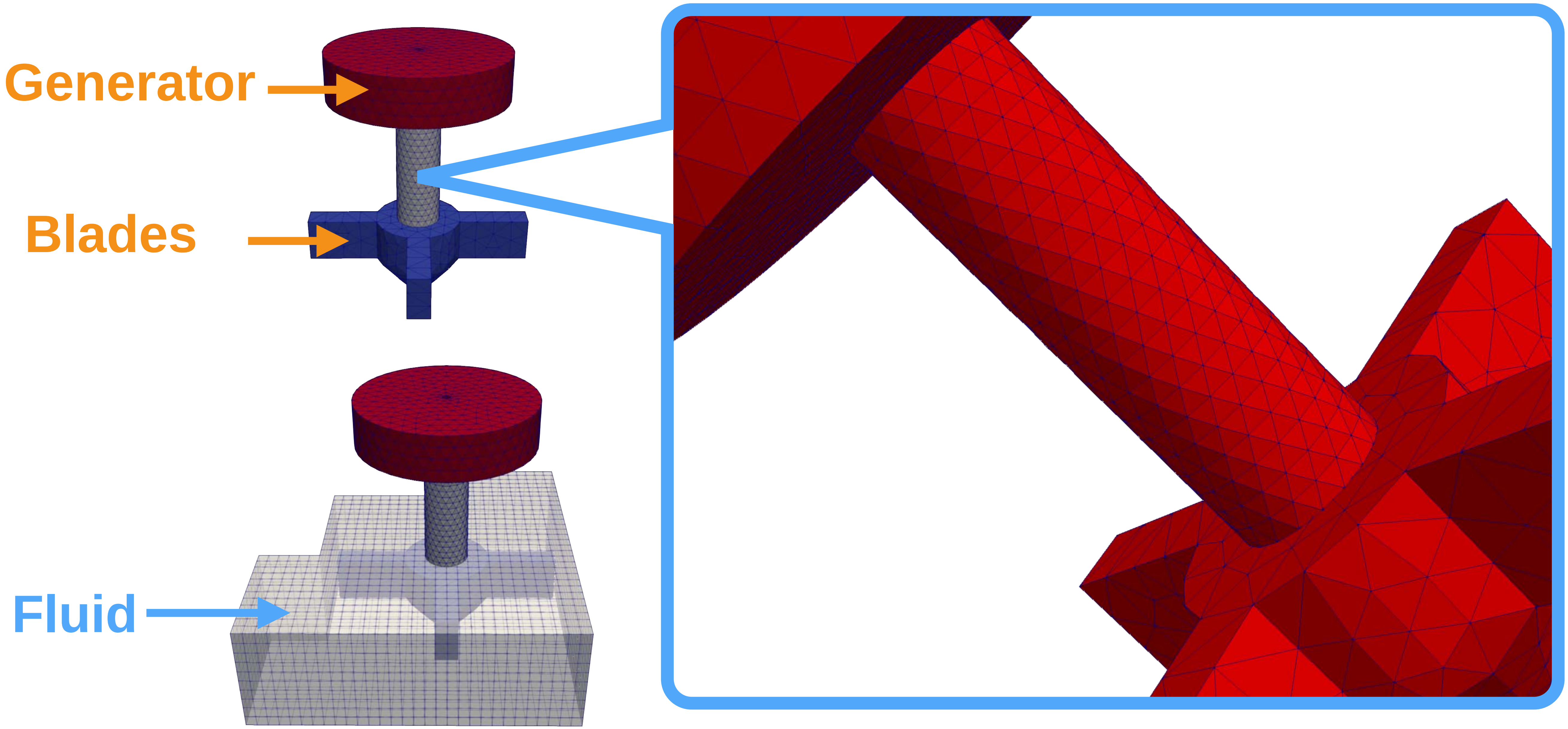

Proof of concept

Mesh-tying and FSI on idealised turbines (2)

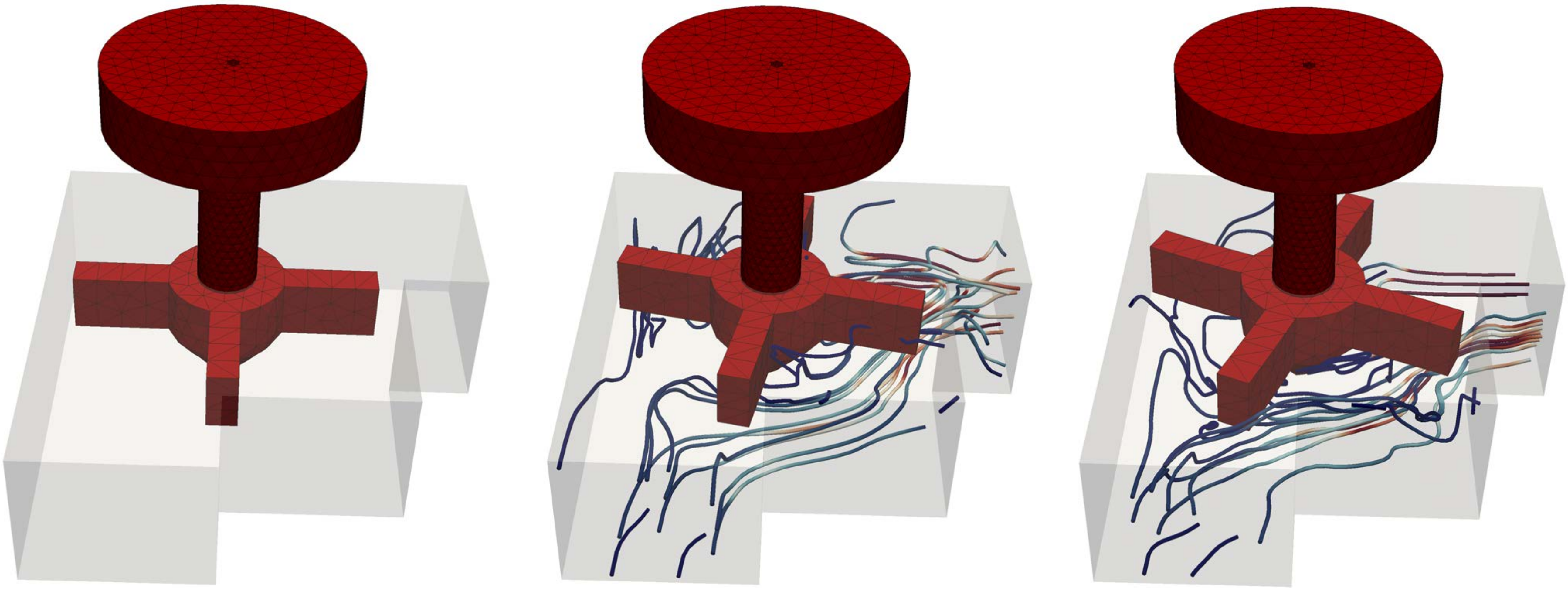

Numerical examples

FSI in rough rock fractures (set-up)

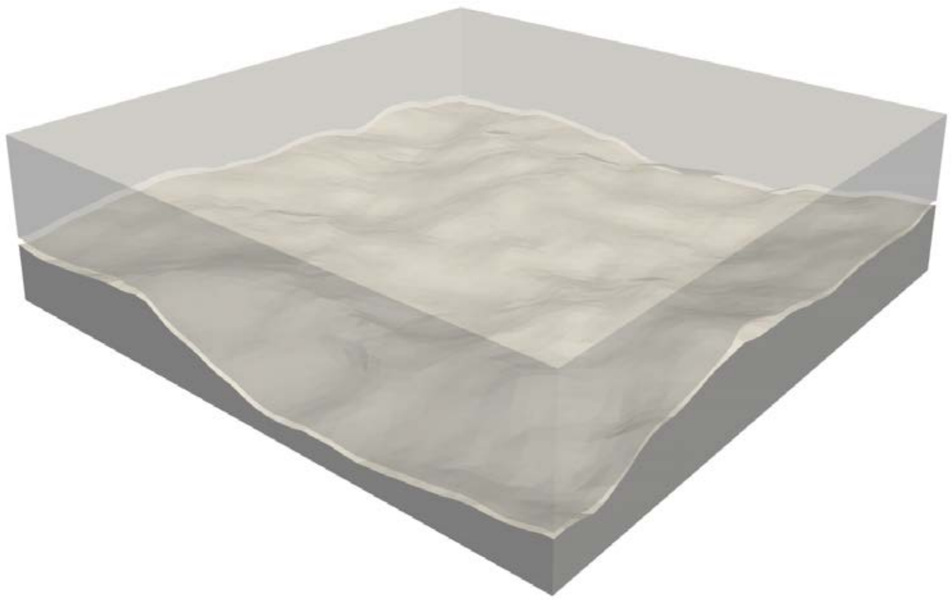

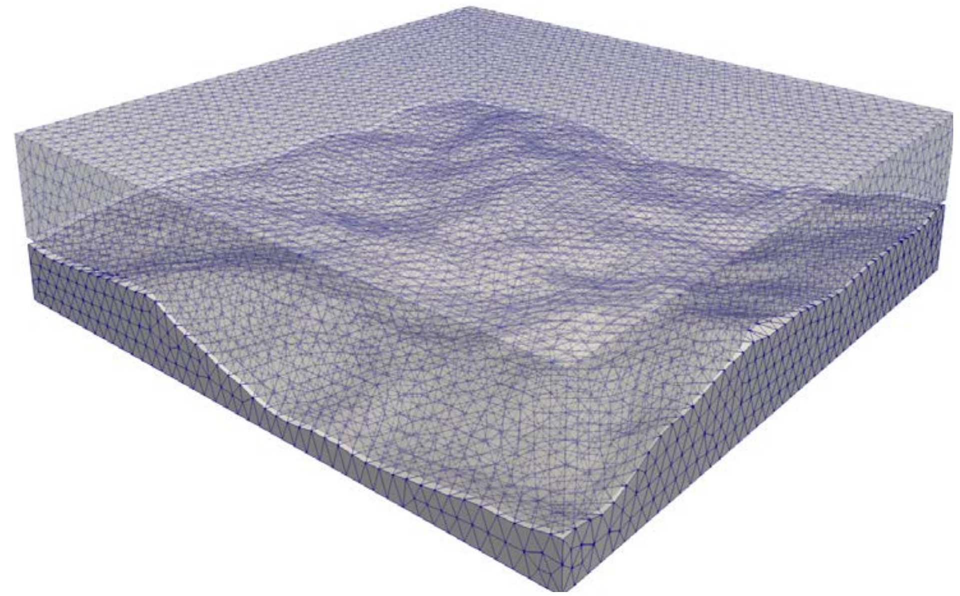

Solid

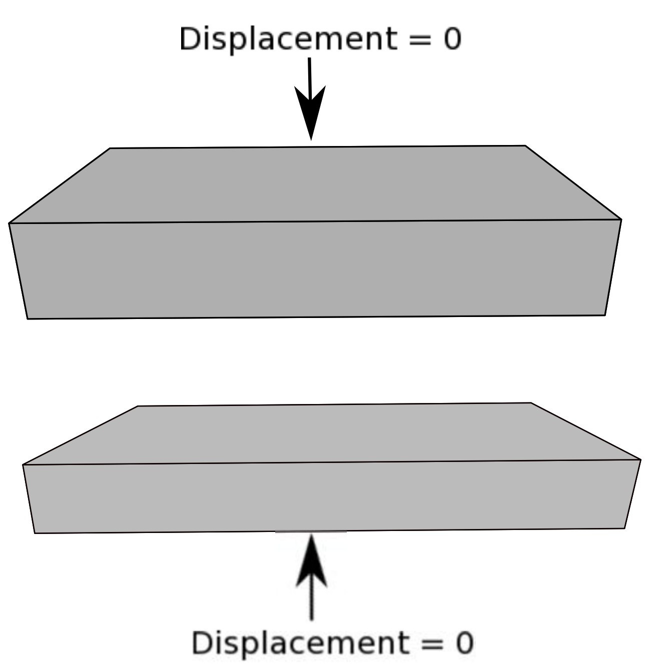

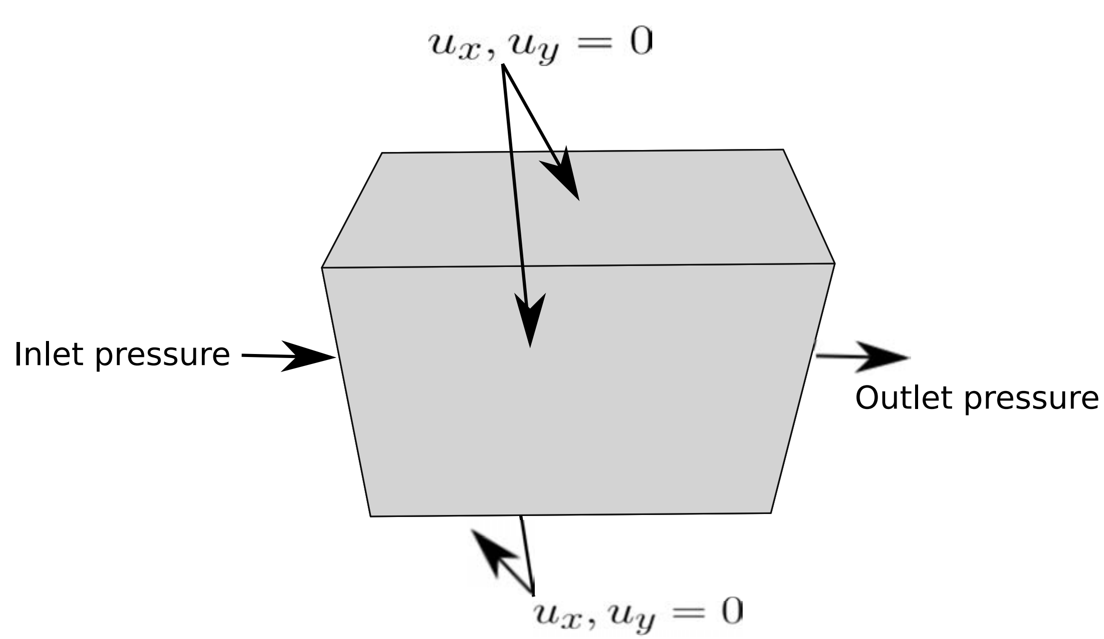

Fluid

Literature: C. v. Planta and others. **Simulation of hydro-mechanically coupled processes in rough rock fractures using an immersed boundary method and variational transfer operators**. To be submitted.

Numerical examples

FSI in rough rock fractures

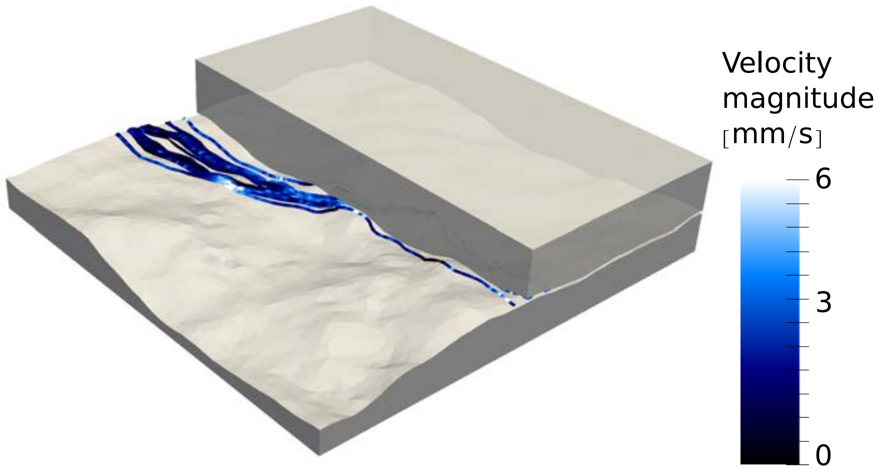

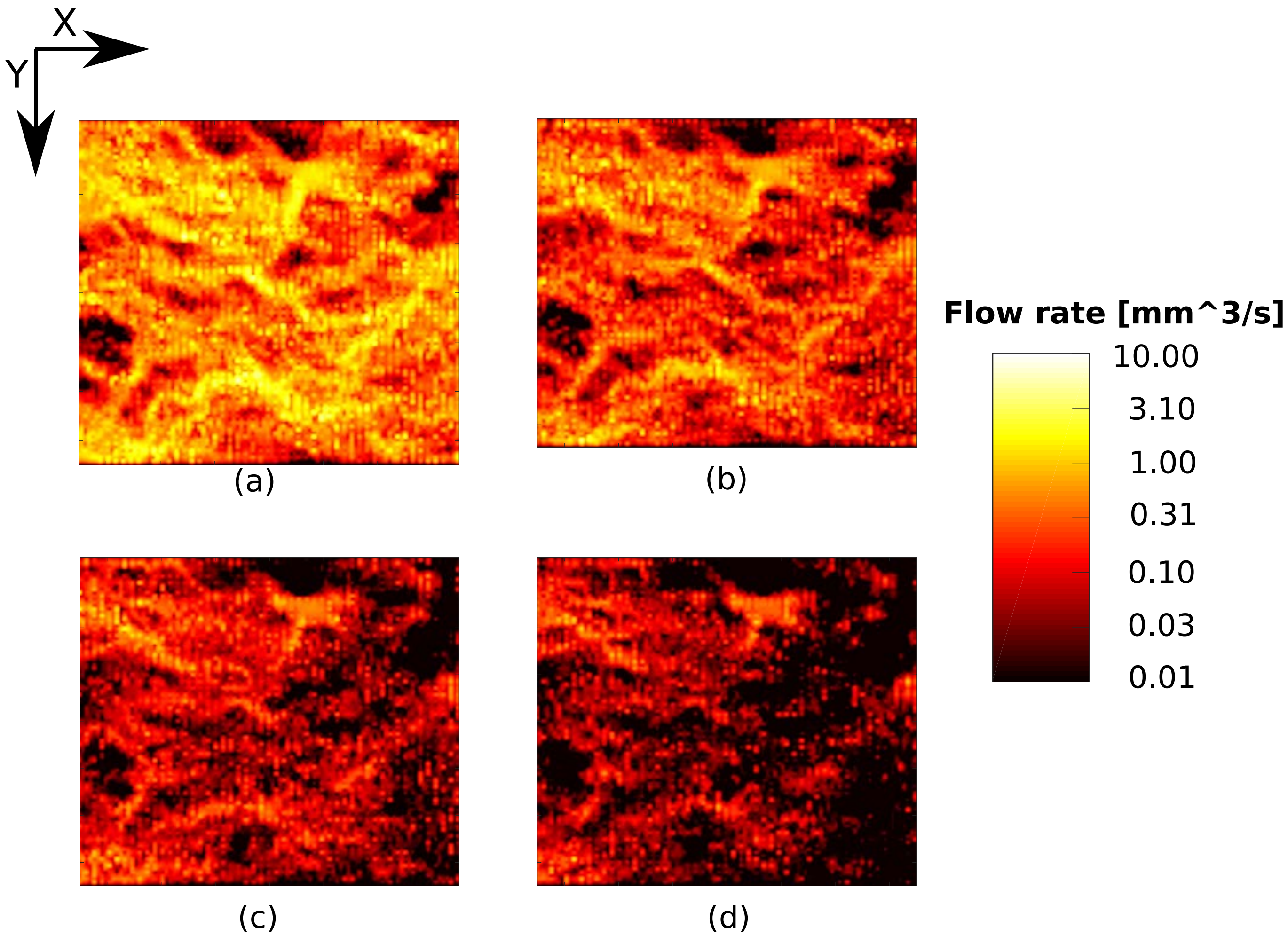

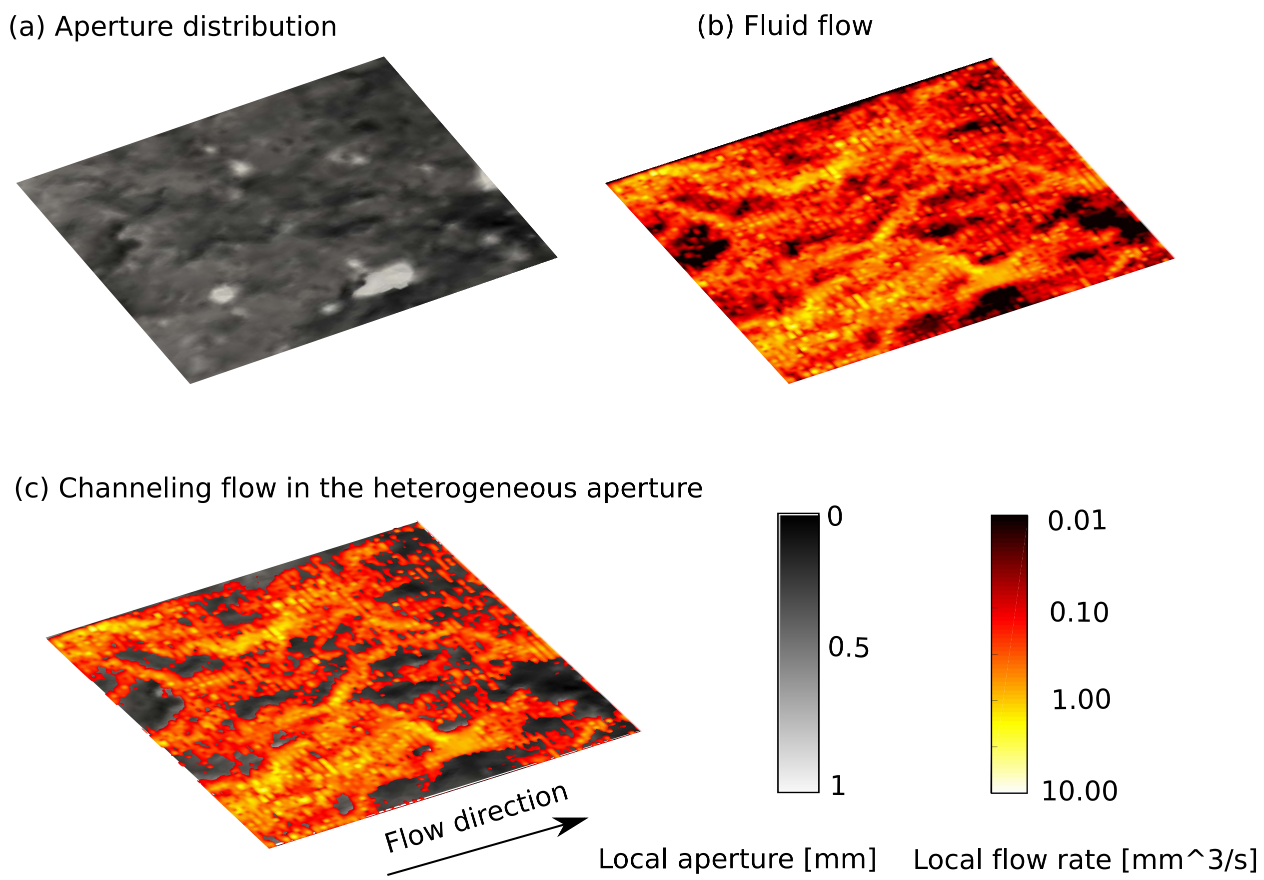

Fluid-saturated fractured porous rocks

Seismic wave propagation ⇒ Fluid pressure diffusion at mesoscale ⇒ Attenuation and velocity dispersion

Boundary conditions — Biot's equations — Output

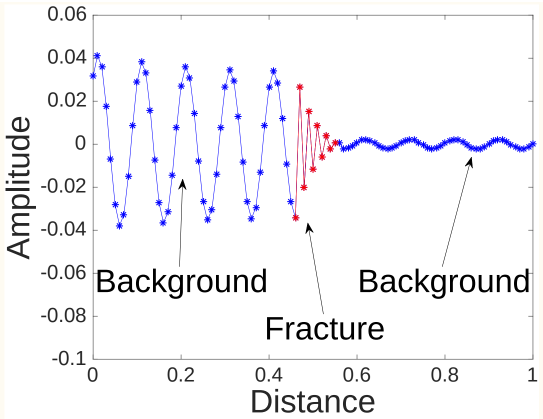

⇓

geometric + mechanical + hydraulic properties of fracture networks in rock formations

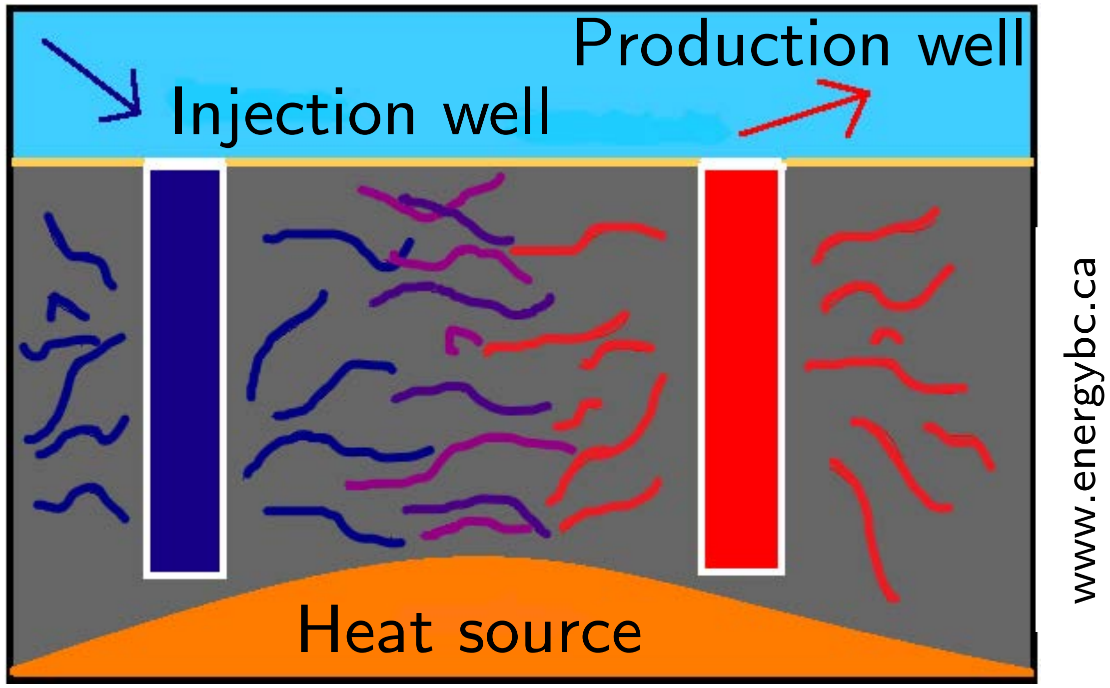

Fractures as fluid pathways

Hydro-mechanical coupled models

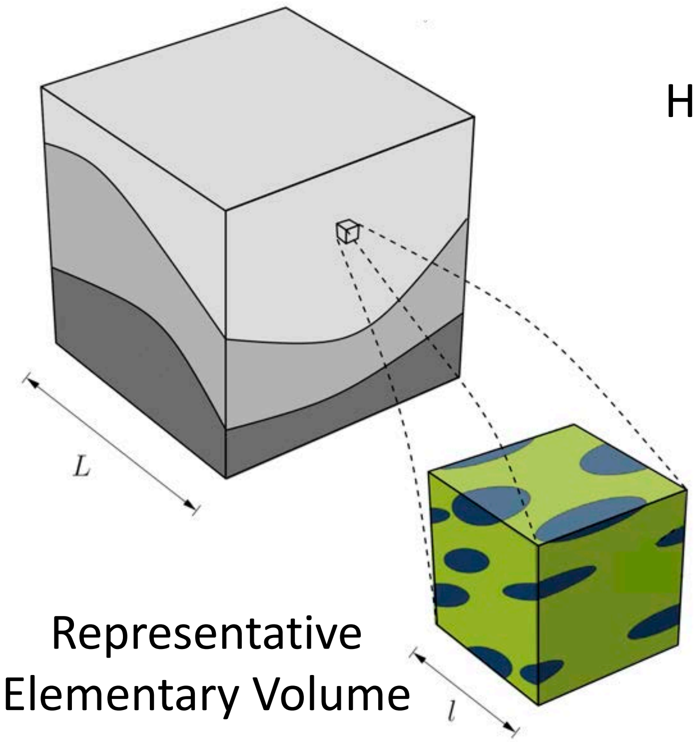

Representative Elementary Volume

Homogeneous macroscale:
visco-elastic model

Upscaling

Heterogenous mesoscale:
large contrast
in material properties
(permeability, stiffness, ...)

Adapted from Jänicke et al. (2015)

Numerical Upscaling Experiments

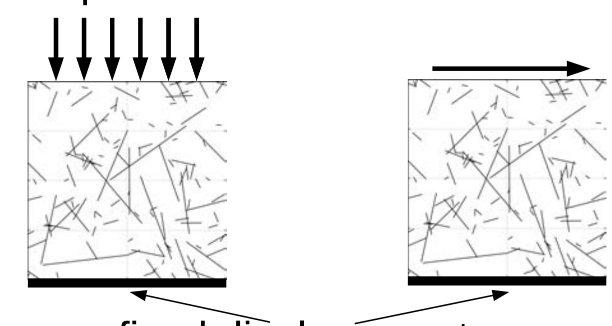

periodic: displacement, stress, fluid pressure and the flux of the pore fluid

$\Downarrow$

to evaluate frequency-dependent

- attenuation
- velocity dispersion

$\Big\} \; Y_\omega$

Hybrid-dimensional model:
lower dimensional fractures

- simplified physics
- simple geometries

Biot's equations:
"thick" fractures ✓

- complete coupled physics
- complex fracture geometries

Mathematical framework for homogenisation

Fracture distribution in a Representative Elementary Volume

- deterministic information not available or insufficient ✗
- statistical properties ✓

Monte Carlo method: N samples to estimate $\mathbb{E}(Y_\omega)$

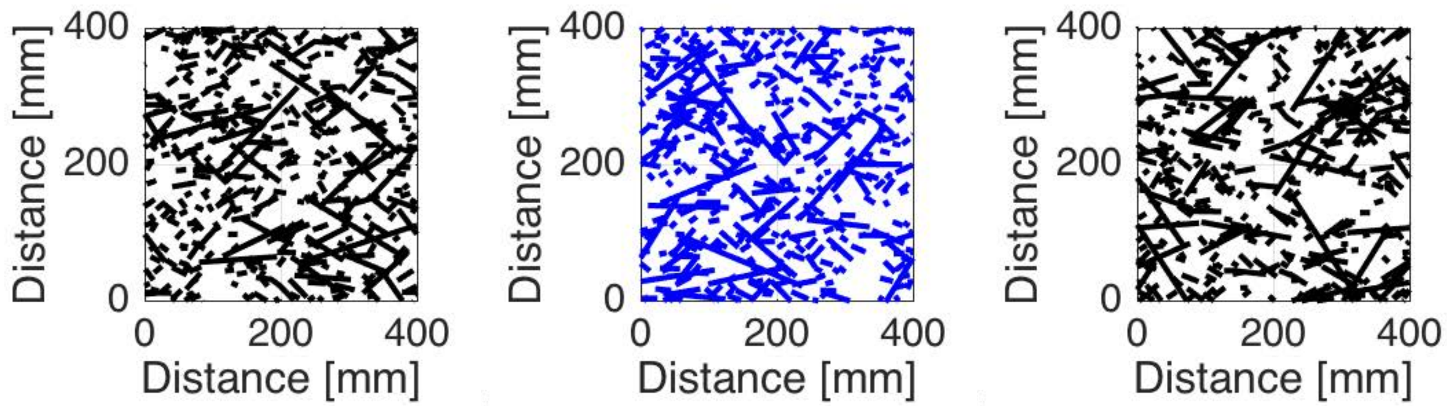

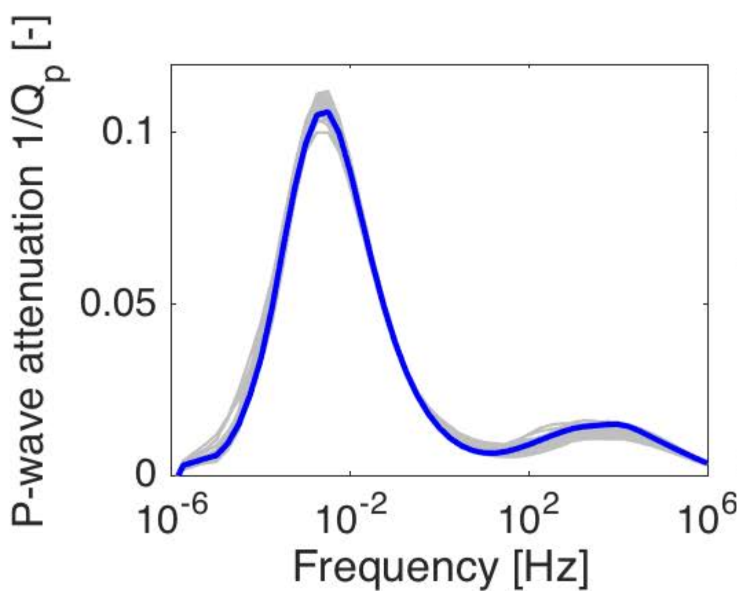

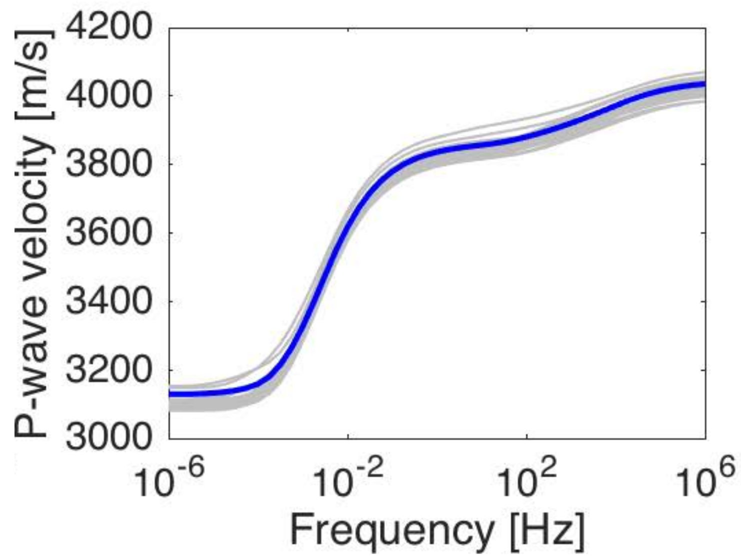

Monte Carlo approximation

$$\frac{1}{N}\sum_{n=1}^{N} Y_\omega^n$$

Adaptive algorithm for mesh generation

Multi-scale problem

- Fracture thickness *0.1%* of domain size
- 50 to 200 fractures
- **Conforming mesh generation**
  - Hands-on
  - Time consuming
- **Adaptive mesh-refinement**
  - Automatic
  - Complex fracture networks

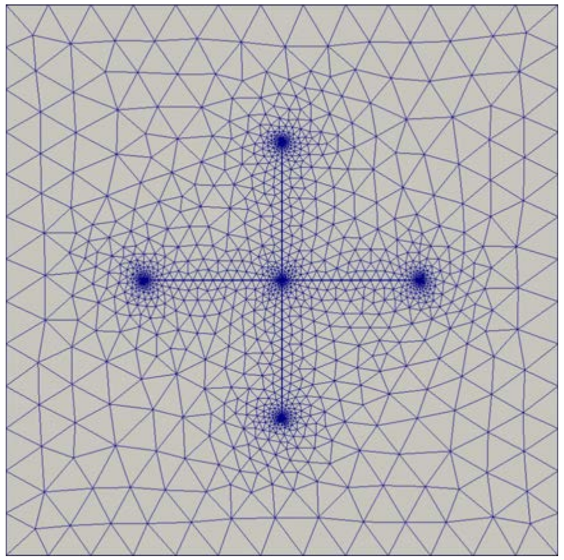

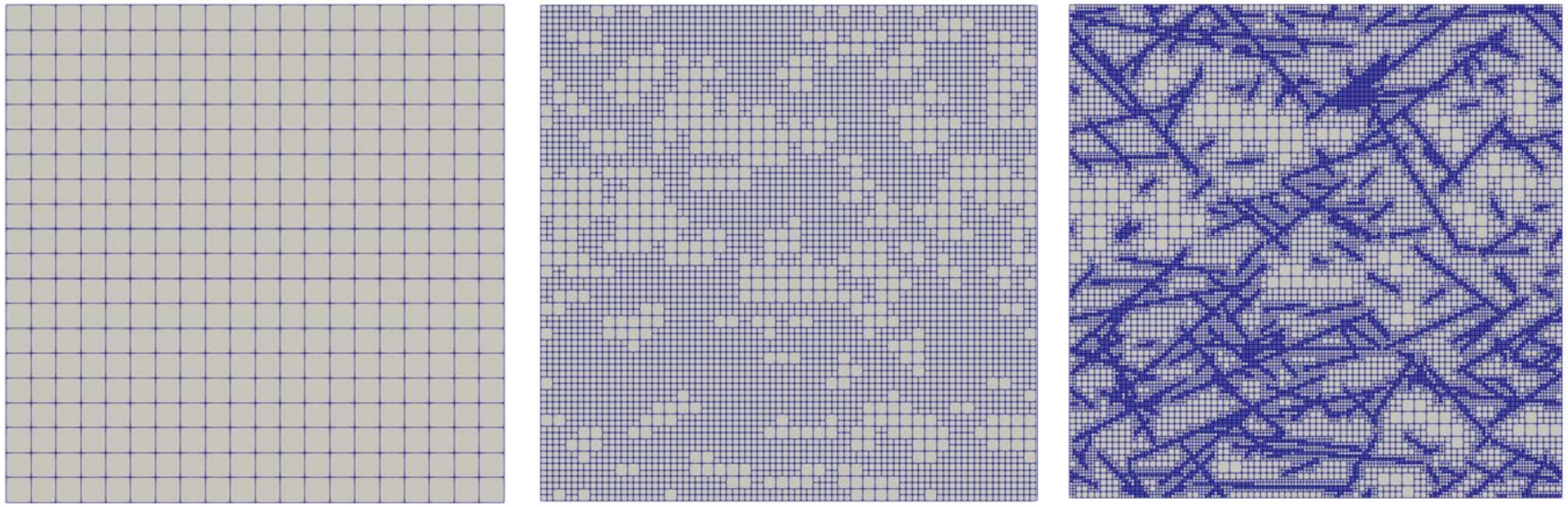

Literature: Burstedde et al. 2011

Validation

Convergence to analytical solution

- No difference between adaptive (**2.9 M nodes**) and uniform refinement (**135 M nodes**) for same minimum mesh size

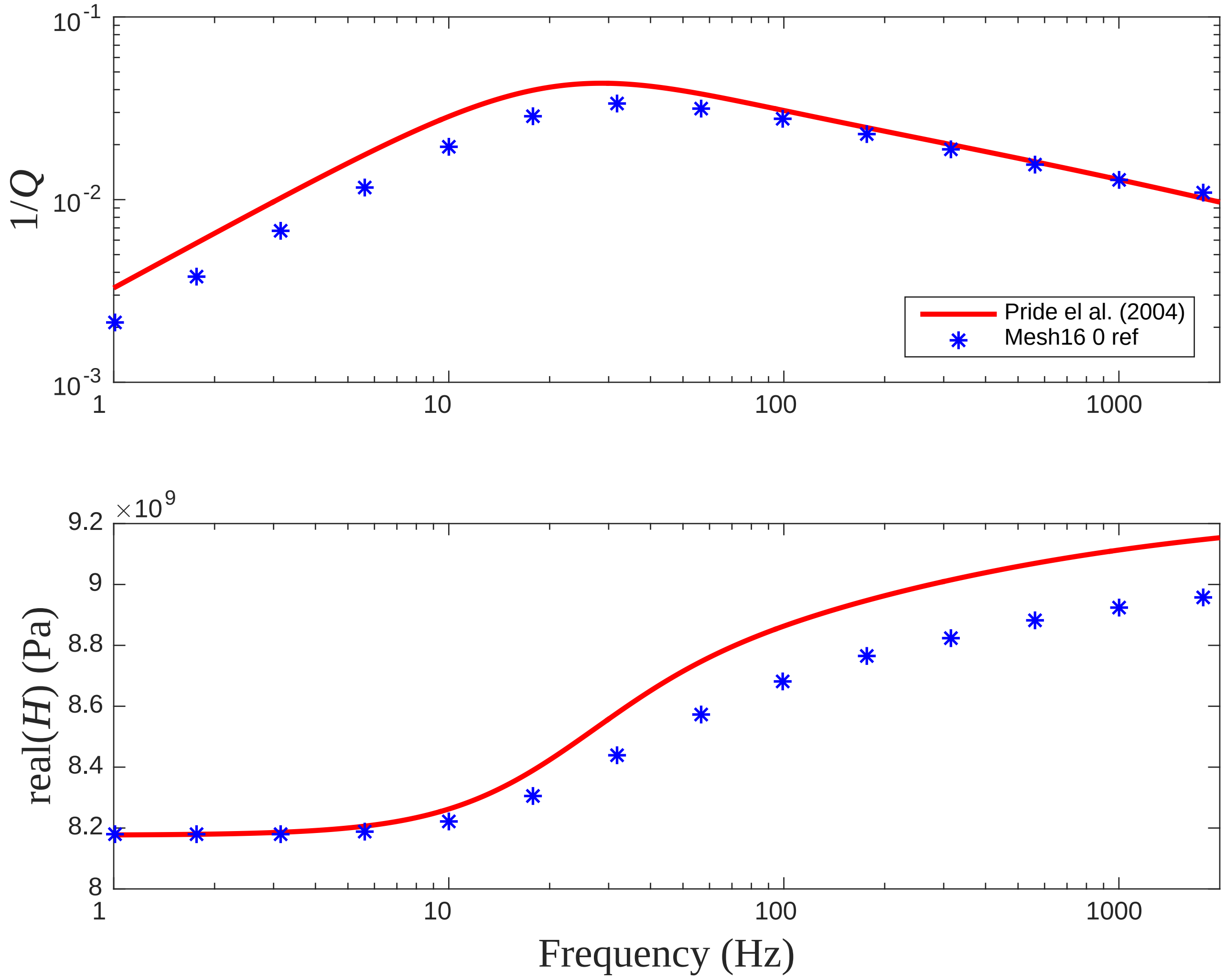

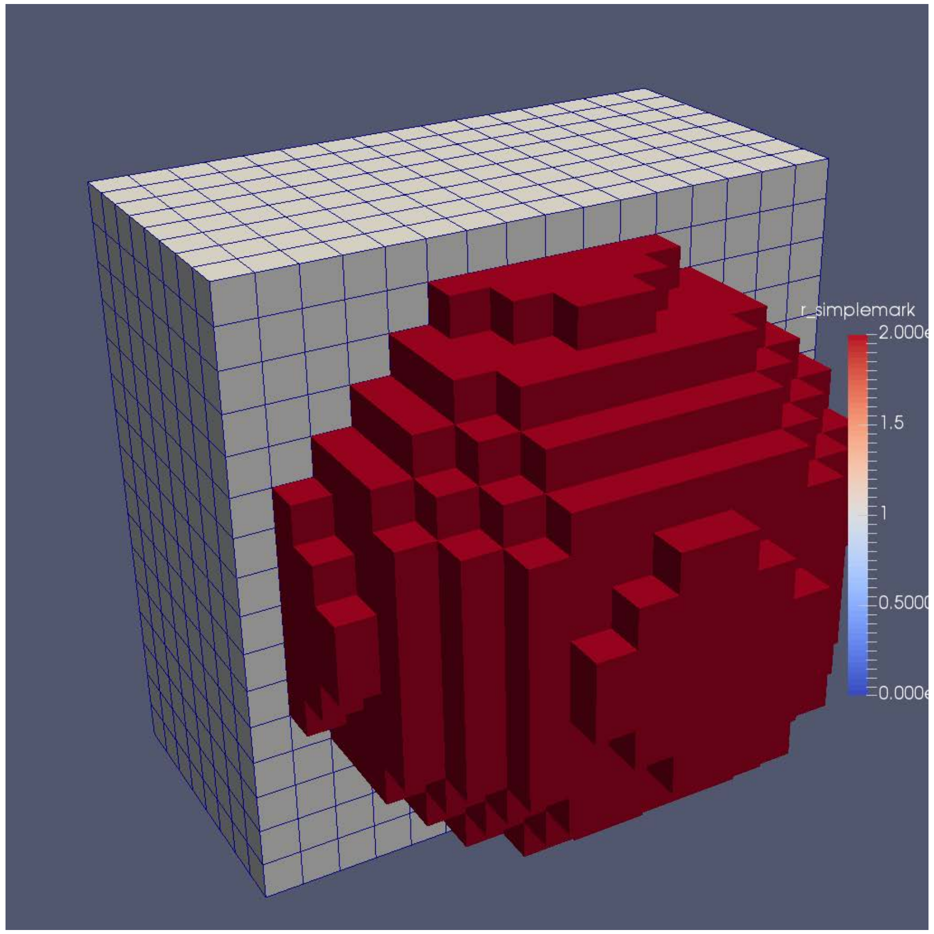

Validation

Convergence to analytical solution

- No difference between adaptive (**2.9 M nodes**) and uniform refinement (**135 M nodes**) for same minimum mesh size

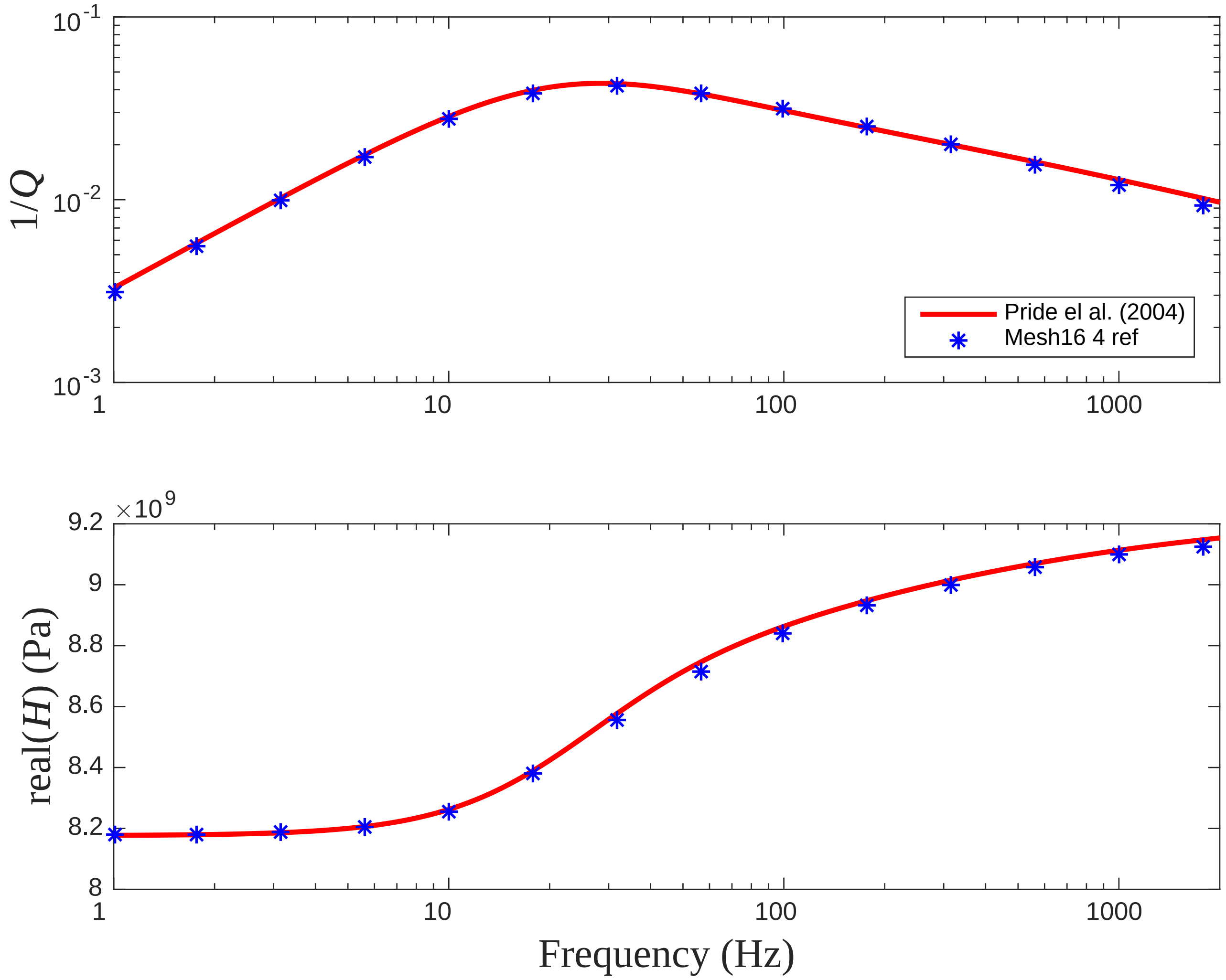

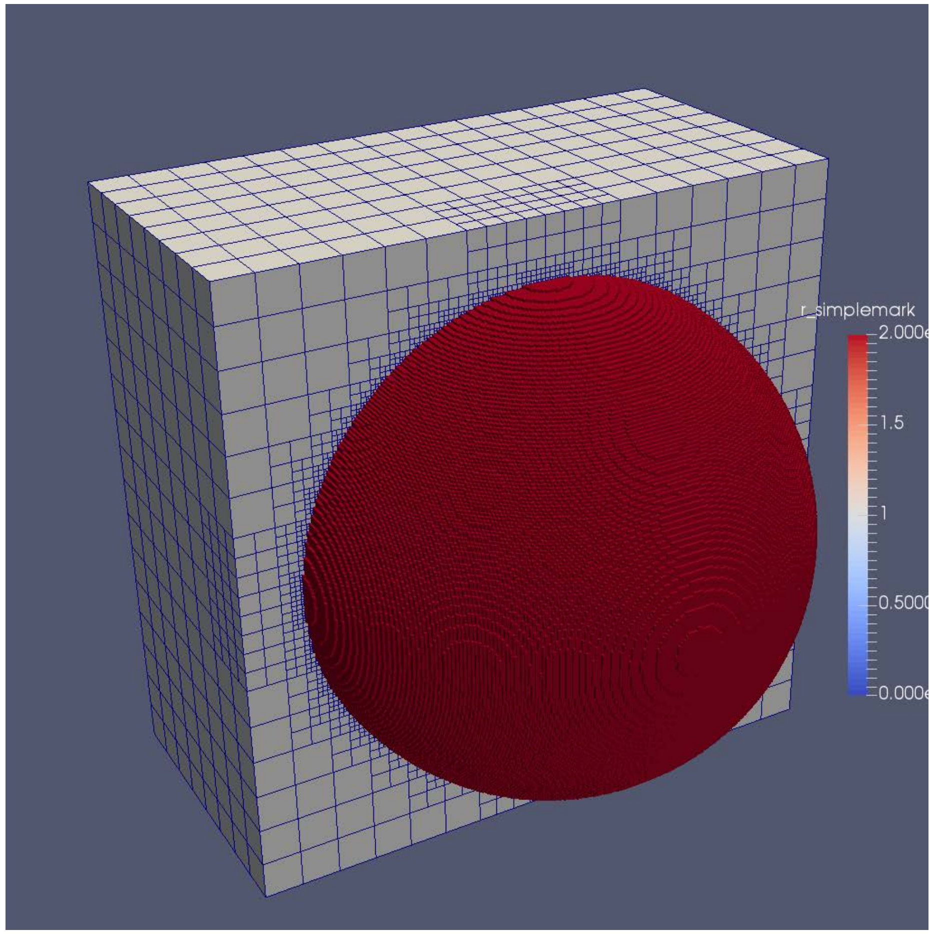

Cascadic multigrid (preliminary results)

Sequence of solution exploiting refinement levels

- Solution for coarsest space
- Coarse space solution is projected (**L^2 –projection**) onto the fine-space
- 3-post-smoothing steps of Block-Gauss-Seidel algorithm

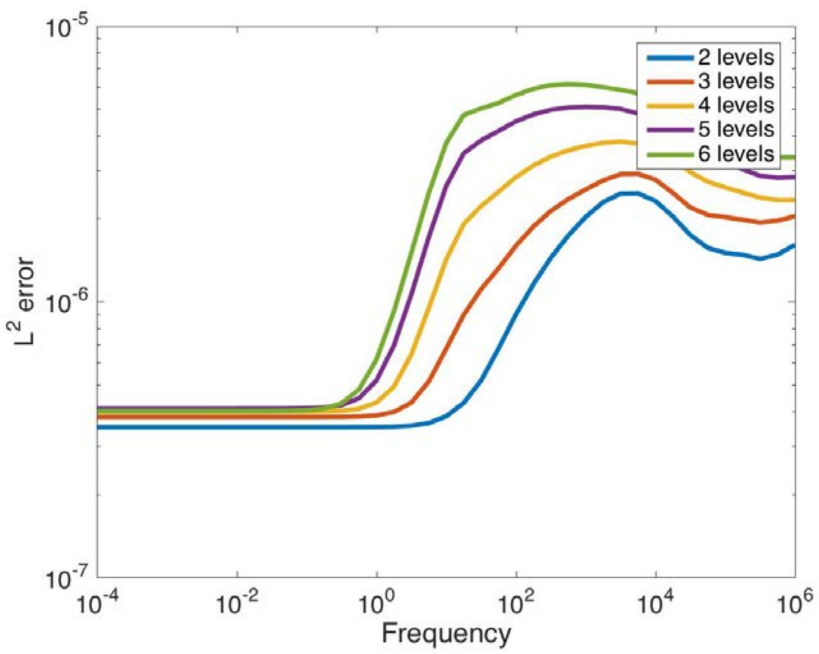

L^2—error direct solver vs. MG

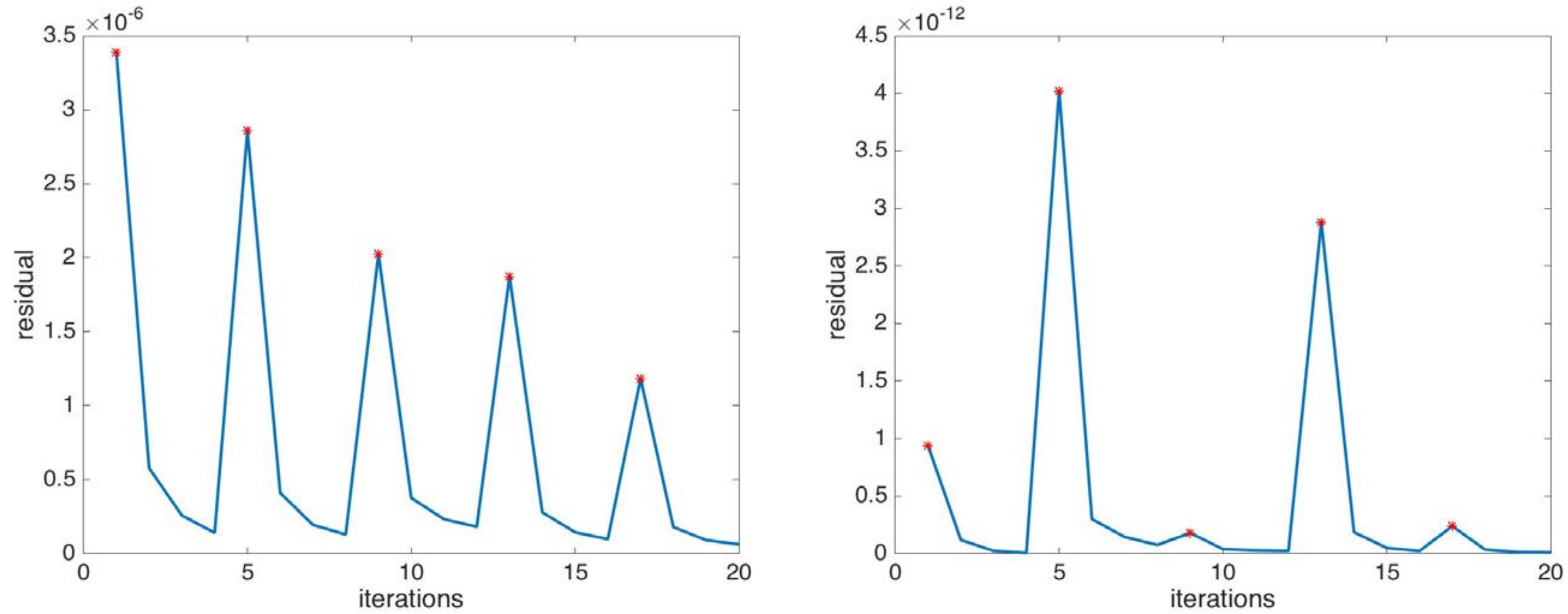

Residual—error history low freq — high freq

Cascadic multigrid (preliminary results)

Adaptivity and low-cost MG strategy and **uniform and direct solver strategy** provide same P-wave attenuation and velocity dispersion curves

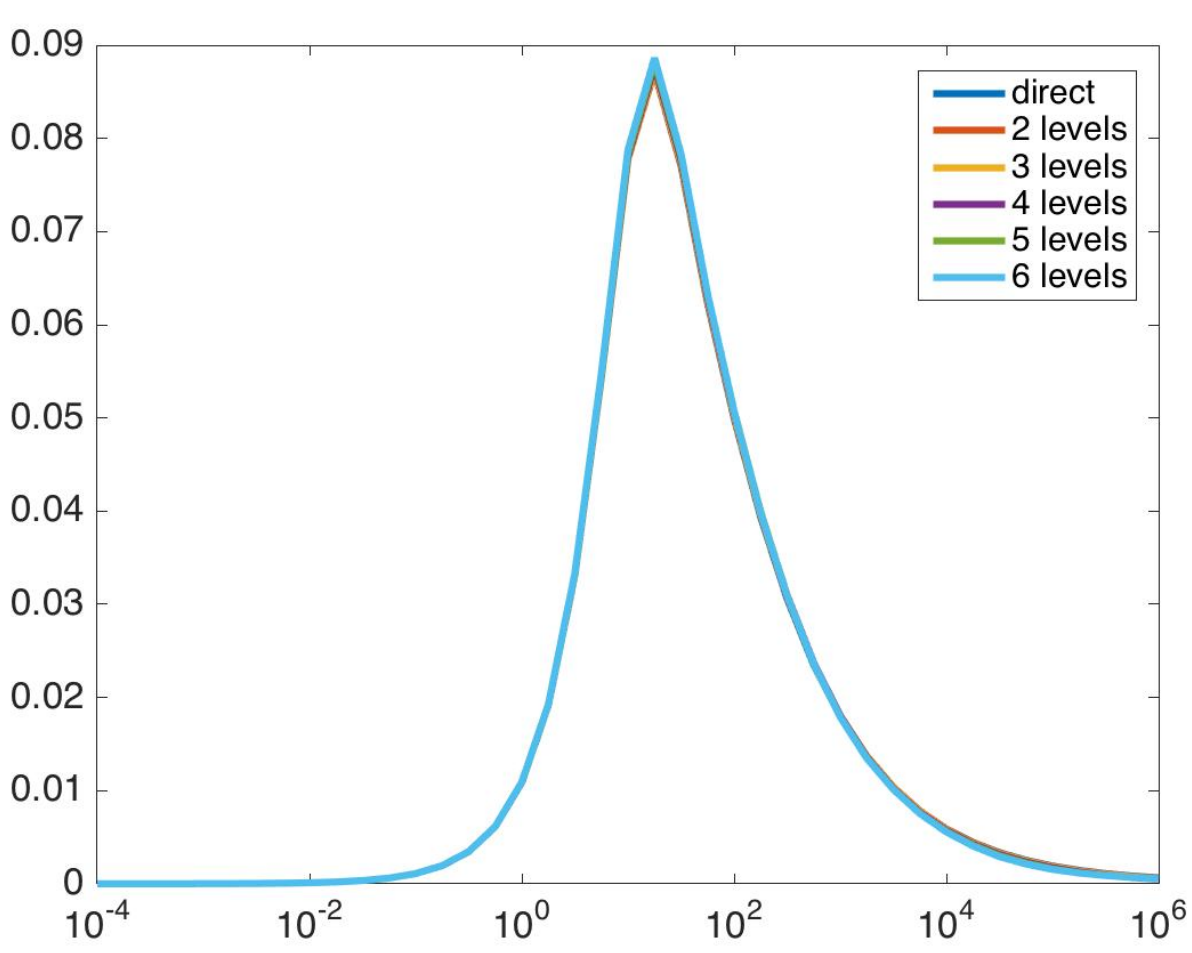

P-wave attenuation

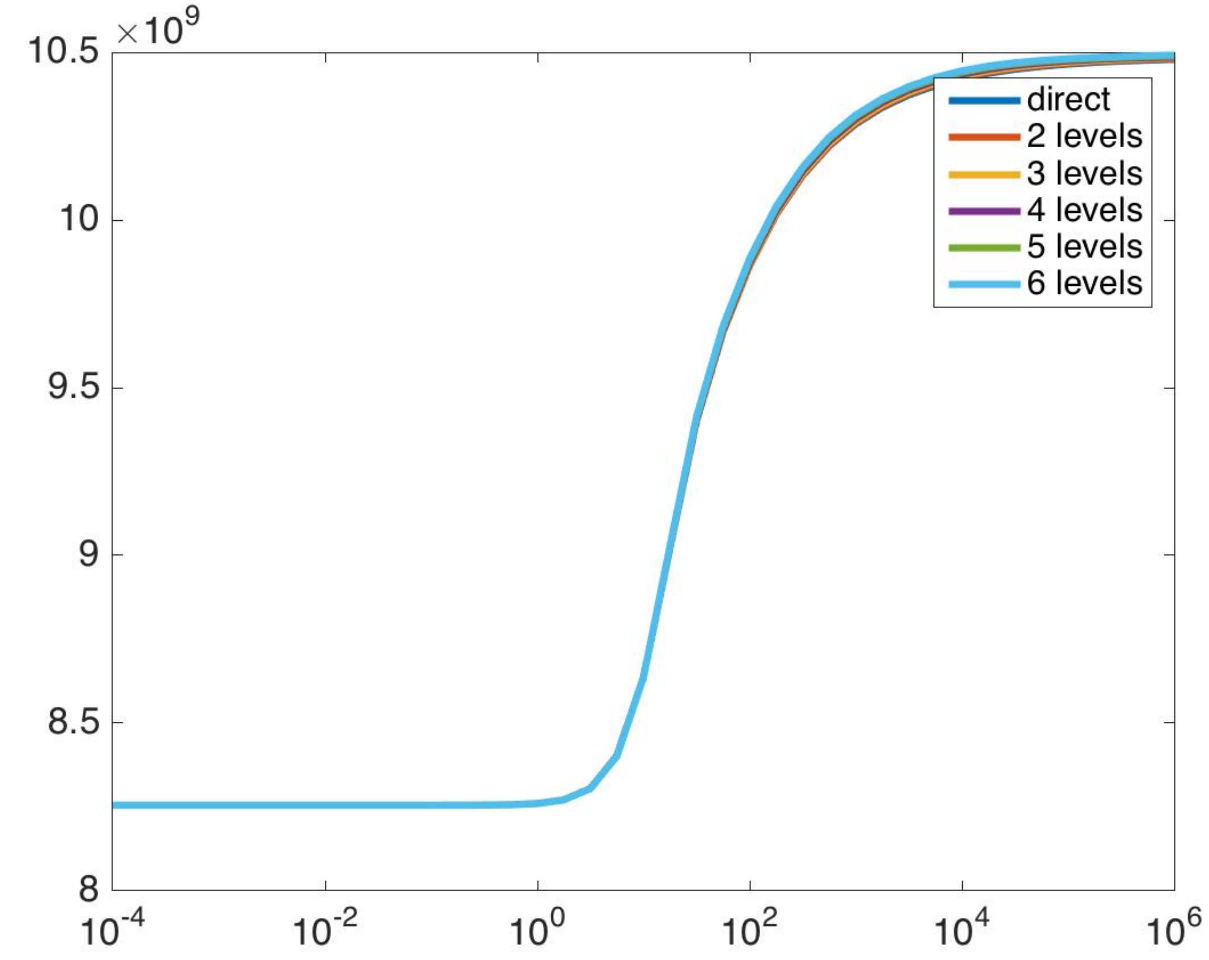

Velocity dispersion

Publicly available codes

In collaboration with

CSCS
Centro Svizzero di Calcolo Scientifico
Swiss National Supercomputing Centre

Utopia	bitbucket.org/zulianp/utopia
ParMOONoLith	bitbucket.org/zulianp/par_moonolith
MFEM-MOONoLith	github.com/mfem/mfem/tree/moonolith-dev

In collaboration with

Lawrence Livermore National Laboratory

Conclusions

Presented today

- **Fictitious domain**/mortar element method for FSI
- Parallel **L^2—projection** for volume and surface coupling
- **Multilevel** method for **stochastic fracture** networks, validated for sphere inclusion

Software

- **Moonolith + Utopia** (L2—projections)
- **Parrot** (Poro-elasticity for fractures)
- **MOOSE** (FEM)

Future work

- **Multigrid** method for realistic fracture networks and **Multilevel Monte Carlo**

Thank you for your attention

See you in Lugano at

Università della Svizzera italiana
Institute of Computational Science ICS

X-DMS 2019

eXtended Discretization MethodS

Important Dates

Opening of minisymposia proposals	August 15, 2018
Minisymposia acceptance notification	November 15, 2018
Opening of abstract submissions	November 15, 2018
Deadline for abstract submissions	January, 15, 2019
Abstract acceptance notification	February 15, 2019

Articles related to this talk

A Parallel Approach to the Variational Transfer of Discrete Fields between Arbitrarily Distributed Unstructured Finite Element Meshes. Rolf Krause and Patrick Zulian. SIAM Journal on Scientific Computing, 2016.

An immersed boundary method based on the L2-projection approach. Maria Giuseppina Chiara Nestola, Barna Becsek, Hadi Zolfaghari, Patrick Zulian, Dominik Obrist, and Krause Rolf. Proceedings of the 24rd International Conference on Domain Decomposition Methods, 2018.

An immersed boundary method for fluid-structure interaction based on overlapping domain decomposition. Maria Giuseppina Chiara Nestola, Barna Becsek, Hadi Zolfaghari, Patrick Zulian, Dario Demarinis, Dominik Obrist, and Krause Rolf. Journal of computational physics (in review).